Acta Pharmaceutica Sinica B 2023;13(1):82–99

Chinese Pharmaceutical Association
Institute of Materia Medica, Chinese Academy of Medical Sciences

Acta Pharmaceutica Sinica B

www.elsevier.com/locate/apsb
www.sciencedirect.com

ORIGINAL ARTICLE

# Bispecific sigma-1 receptor antagonism and mu-opioid receptor partial agonism: WLB-73502, an analgesic with improved efficacy and safety profile compared to strong opioids

**Alba Vidal-Torres, Begoña Fernández-Pastor, Mónica García, Eva Ayet, Anna Cabot, Javier Burgueño, Xavier Monroy, Bertrand Aubel, Xavier Codony, Luz Romero, Rosalía Pascual, Maria Teresa Serafini, Gregorio Encina, Carmen Almansa, Daniel Zamanillo, Manuel Merlos, José Miguel Vela***

*WeLab Barcelona, Parc Científic de Barcelona, Barcelona 08028, Spain*

Received 13 April 2022; received in revised form 17 June 2022; accepted 18 July 2022

**KEY WORDS**

WLB-73502;
Sigma-1 receptor;
Mu-opioid receptor;
Biased agonist;
Analgesic activity;
Chronic pain;
Neuropathic pain;
Safety

**Abstract** Opioids are the most effective painkillers, but their benefit-risk balance often hinder their therapeutic use. WLB-73502 is a dual, bispecific compound that binds sigma-1 (S1R) and mu-opioid (MOR) receptors. WLB-73502 is an antagonist at the S1R. It behaved as a partial MOR agonist at the G-protein pathway and produced no/unsignificant $\beta$-arrestin-2 recruitment, thus demonstrating low intrinsic efficacy on MOR at both signalling pathways. Despite its partial MOR agonism, WLB-73502 exerted full antinociceptive efficacy, with potency superior to morphine and similar to oxycodone against nociceptive, inflammatory and osteoarthritis pain, and superior to both morphine and oxycodone against neuropathic pain. WLB-73502 crosses the blood–brain barrier and binds brain S1R and MOR to an extent consistent with its antinociceptive effect. Contrary to morphine and oxycodone, tolerance to its antinociceptive effect did not develop after repeated 4-week administration. Also, contrary to opioid comparators, WLB-73502 did not inhibit gastrointestinal transit or respiratory function in rats at doses inducing full efficacy, and it was devoid of proemetic effect (retching and vomiting) in ferrets at potentially effective doses. WLB-73502 benefits from its bivalent S1R antagonist and partial MOR agonist nature to provide an improved antinociceptive and safety profile respect to strong opioid therapy.

*Corresponding author. Tel.: + 34 618734099.
E-mail address: jvela@welab.barcelona (José Miguel Vela).

Peer review under responsibility of Chinese Pharmaceutical Association and Institute of Materia Medica, Chinese Academy of Medical Sciences.

https://doi.org/10.1016/j.apsb.2022.09.018

## 1. Introduction

Chronic pain is one of the most common health problems worldwide[1]. Despite its large prevalence, chronic pain is still poorly understood and difficult to treat. Pharmacological activation of opioid receptors, particularly the $\mu$-opioid receptor (MOR), is one of the main treatment options. However, the use of opioids is associated with a wide range of side effects including constipation, nausea, vomiting, respiratory depression and dysphoria or euphoria[2]. In addition, under repeated administration, tolerance develops that results in a diminished effectiveness against chronic pain conditions[3]. Analgesic tolerance leads to the use of higher drug doses that increase overdose risk. Due to their reinforcement properties, opioids have a high potential for causing addiction, as proven by the opioid abuse/misuse epidemics (opioid crisis) affecting the United States[4]. Because of the negative aspects of their use, new opioids drug discovery focuses on the design of compounds having greater safety/efficacy ratio[5].

One approach consists in the development of MOR agonists with low intrinsic activity as safer alternatives[6]. However, the reduced side effects often run parallel to limited analgesia and potential advantages of partial opioid agonists are not clearly borne out in clinical practice[7]. In the case of buprenorphine, a non-selective schedule III partial MOR agonist (also binds to kappa and delta opioid receptors), analgesia is remarkable and some responder and safety analyses[8], and benefit-risk assessments[9] support its use over full MOR agonists for chronic pain treatment.

Alternative approaches include biased ligands that promote preferential signalling through one of the MOR transducers[10]. This concept generated considerable excitement as the $G_{i/o}$ protein pathway was proposed to mediate analgesia while the $\beta$-arrestin pathway the opioid-related adverse effects[11]. Oliceridine (TRV130, Olinvyk®, Trevena, Inc., King of Prussia, PA, USA), a G-protein-biased MOR agonist indicated for intravenous treatment of acute pain was reported to exhibit a favourable safety profile compared to morphine[12]. However, oliceridine produces typical opioid abuse-related effects in rodents and humans[13]. Confirmation of its improved benefit-risk profile would probably require specific trials examining its safety *versus* conventional opioids[14].

The benefit-risk of opioid analgesics may also be improved by multimodal mechanisms, combining opioid and non-opioid pathways to enhance efficacy and/or minimize adverse effects[15,16]. Innovation in multimodal analgesia involving opioid mechanisms goes from i) free combinations (2 tablets, 2 active ingredients; polypharmacy, frequent in clinical practice); ii) to fixed-dose combination formulations (1 tablet, 2 active ingredients; *e.g.*, tramadol/acetaminophen)[17]; iii) to drug−drug co-crystals (1 tablet, 2 active ingredients non-covalently bonded in a co-crystal lattice; *e.g.*, Seglentis®, a co-crystal of tramadol and celecoxib)[18,19]; and finally iv) to multimodal drugs (1 tablet, 1 active ingredient with at least 2 activities; *e.g.*, Nucynta®, tapentadol, a MOR agonist and norepinephrine reuptake inhibitor)[20]. The discovery of single compounds that bind to two distinct targets, also known as dual, bivalent, bifunctional or bispecific ligands, is challenging, but such drugs offer advantages respect to drug combinations besides improved efficacy and/or safety. These include superior patient compliance with medication (one instead of various pills at potentially different dosage frequencies), lower risk of drug−drug interactions, simpler (single) pharmacokinetics and synchronic/overlapping engagement of targets, and less variability among patients, both in drug exposure and response to treatment[21]. The non-opioid mechanism should ideally have an independent effect and synergistic analgesic activity when used with opioids, but it should not enhance or preferably counteract opioid-related side effects. This is the case of the sigma-1 receptor (S1R, $\sigma_1$R) antagonism mechanism. Based on drug combination studies, S1R antagonists increase the therapeutic index of opioids by enhancing analgesia[22,23] and adding a unique analgesic action in "opioid-resistant pain", particularly neuropathic pain[24]. Besides inhibition of pain hypersensitivity *per se*, S1R antagonists "release the brake" enabling opioids to exert enhanced antinociceptive effects[25,26] as S1R is a tonically active system limiting opioid analgesia[22]. Potentiation of opioid analgesia by S1R blockade results in an opioid-sparing effect at equianalgesia, which translates into improved safety of the combination compared to opioid monotherapy. Contrary to analgesia, opioid side effects are not potentiated and some of them are counteracted[22,23,26,27], which further contributes to a better safety profile of the combination.

A drug discovery program was undertaken to identify a multimodal, bispecific drug with S1R and MOR activities using a pharmacophore merging approach, which led to the discovery of WLB-73502[28]. Here we disclose the pharmacological *in vitro* and *in vivo* efficacy and safety profile of WLB-73502 in comparison with strong opioids (morphine and oxycodone). Results are discussed according to their potential as a replacement alternative to strong opioid monotherapy.

## 2. Materials and methods

### 2.1. *In vitro studies*

#### 2.1.1. *Functional profile on MOR*

Cyclic 3′,5′-adenosine monophosphate (cAMP) measurements on CHO-K1 cells that stably express the human MOR (PerkinElmer ES-542-C; Waltham, MA, USA) were performed using a system based on Homogeneous Time Resolved Fluorescence. The cAMP Kit (CisBio, 62AM4PEJ; Codolet, France) was used according to the manufacturer's recommendation. 2500 cells/well were seeded the day before the experiment in Opti-Mem (Gibco, 11058-021; Amarillo, TX, USA). Opioid agonists were prepared in Opti-Mem with 3-isobutyl-1-methyl-xanthine (Sigma−Aldrich, I5879-5G; Burlington, MA, USA) and forskolin (Tocris, 1099; Bristol, UK) at 0.5 mmol/L and 7.5 μmol/L respectively and added to the cells. After 45 min at 37 °C the reaction was stopped by lysing the cells. Plates were incubated for an additional hour at room temperature and read at 665 nm/620 nm using a RubyStar Plate Reader (BMG LabTech; Ortenberg, Germany). For the partial inactivation assays, $\beta$-funaltrexamine ($\beta$-FNX, Sigma−Aldrich) was prepared in Opti-Mem and added to the cells the day after seeding at the

following concentrations (0, 1, 3, 10, 30, 100, and 300 nmol/L) for 2 h. Cells were then washed twice with Opti-Mem, left for 1 h at 37 °C, opioid agonists added, and the reaction proceeded as stated above. DAMGO (Sigma−Aldrich) was used as reference MOR full agonist in this assay.

The $\beta$-arrestin-2 recruitment assay was performed using CHO-K1 cells engineered to co-express the ProLink™ Tagged Human MOR and the Enzyme Acceptor Tagged $\beta$-Arrestin-2 from DiscoverX (93-0213C2; Fremont, CA, USA). 5000 cells/well were seeded in PathHunter Cell Plating Reagent (DiscoverX) into 384 well plates. Twenty-four hours later, the ligands (dissolved in HBSS containing 20 mmol/L Hepes) were added to the plate. DAMGO (Sigma−Aldrich) was used as reference full MOR agonist in this assay. Cells were incubated for 90 min at 37 °C, the Detection Reagent (PathHunter) was then added and the incubation continued at room temperature for 60 min more. Luminescence was recorded in an Envision Reader (PerkinElmer).

#### 2.1.2. *Functional profile on S1R*

Guinea pig brain membrane binding assays for the S1R ($\sigma_1$R) using [$^3$H](+)-pentazocine (PerkinElmer) as radioligand were conducted either in the absence or presence of 1 mmol/L phenytoin (DPH) (Sigma−Aldrich), as previously described[29], to identify the functional (agonistic or antagonistic) nature of WLB-73502. Dextromethorphan (Sigma−Aldrich) and haloperidol (Sigma−Aldrich) were used as control, prototypical S1R agonist and antagonist, respectively.

### 2.2. *In vivo studies*

#### 2.2.1. *Animals*

Male Wistar rats (Harlan Laboratories, later Envigo; Milano, Italy), weighing 75−100 g on arrival, and male ferrets (*Mustela putorius furo*) (Marshall BioResources; North Rose, NY, USA), weighing 1000−1800 g, were used. Experimental research in rats was conducted in accordance with the Care and Use of Laboratory Animals Guidelines of the European Community (European Directive 2010/63/EU), with protocols approved by the local Committee of Animal Use and Care, and with ethical standards for investigations of experimental pain[30]. Rats were housed in groups of four, had free access to food and water and were kept in controlled laboratory conditions with temperature maintained at 21 ± 1 °C and 12 h light/dark cycles (on at 07:00 am and off at 07:00 pm). Before starting the experiments, an acclimatization period of 24 h to the new room allowed animals to stabilize in the new environment promoting both animal welfare and reproducible experimental results. Experiments were carried in a sound-attenuated, air-regulated experimental room. The receptor occupancy study in rats was done at RenaSci Ltd (Nottingham, UK; now part of Signature Discovery), following regulation by the Animals (Scientific Procedures) Act 1986 (amended in 2012) that extend the European Directive 2010/63/EU. The study of emesis in ferrets was done at Syncrosome (Marseille, France) and the experimental protocol was approved by the Animal Ethical Committee (French National Committee N°71) and by the Higher Education and Research Ministry, according to the 2010/63 directive from the EU. Animal studies are reported in compliance with the ARRIVE guidelines 2.0[31].

#### 2.2.2. *Drugs and drug administration*

WLB-73502 [(*R*)-9-(2,5-difluorophenethyl)-4-ethyl-2-methyl-1-oxa-4,9-diazaspiro[5.5]undecan-3-one; formerly identified as EST73502] (Fig. 2B) was synthesized as previously described[28]. All studies were performed with WLB-73502 fumarate salt, except for the emesis study in ferrets that was performed with WLB-73502 hydrochloride salt. Morphine (hydrochloride salt) was supplied by Alcaliber (Madrid, Spain) and oxycodone (hydrochloride salt) by Johnson Matthey (London, UK). WLB-73502, morphine and oxycodone were dissolved in 0.5% hydroxypropyl methylcellulose to their final concentrations immediately before administration. Drugs were administered intraperitoneally (i.p.) or subcutaneously (s.c.) in a volume of 10 or 5 mL/kg, respectively; an equal volume of vehicle (0.5% hydroxypropyl methylcellulose) was used in control animals. In some studies, repeated twice a day (b.i.d.; bis in die) treatments (morning and evening, 8 h apart) were done. Drug doses refer to their base forms. Animals were randomized to groups. The experimenter was blind to the treatment group in all experiments.

#### 2.2.3. *Paw pressure test*

The test was based on the one previously described by Randall and Selitto[32]. Male Wistar rats were gently restrained and an increasing mechanical nociceptive stimulus using a cone-shaped plastic tip (Analgesy-meter, Ugo Basile; Gemonio, Italy) was applied to the dorsal surface of the right hind paw. The paw pressure threshold (PPT) was defined as the pressure (in g) at which the rat voluntarily withdrew the hind paw (struggle response). The test was done twice at an interval of 1 min between each stimulation with a 1000 g cut-off to avoid skin damage. The PPT was calculated as the mean of the two averaged values. Data were presented as PPTs and as percentage of antinociception of treatments respect to vehicle. A total of 77 animals were used to perform acute treatment experiments. No criteria for excluding animals were set and all animals in all experimental groups were included. Rats ($n$ = 7 per group) were randomly allocated to experimental groups to receive i.p. vehicle or different doses of WLB-73502 (1.25, 2.5 and 5 mg/kg), morphine (5, 7.5, 10 and 20 mg/kg) or oxycodone (1.25, 2.5 and 3.75 mg/kg). The PPT was evaluated 20 min after vehicle or drug administration.

#### 2.2.4. *Tail-flick test*

The test was based on that described by D'Amour and Smith[33]. Rats were gently restrained with a cloth to orient their tails toward the source of heat of the tail-flick apparatus (Panlab, LE 7106; Barcelona, Spain). A noxious beam of light was focused on the tail about 5 cm from the tip, and the tail-flick latency (TFL, time between the onset of the radiant heat beam and removal of the tail) was recorded automatically to the nearest 0.1 s. The intensity of the radiant heat source was adjusted to yield baseline latencies between 2 and 5 s and a cut-off time was set at 10 s to avoid heat-related damage. A total of 77 animals were used to perform experiments. No criteria for excluding animals were set and all animals in all experimental groups were included. Rats ($n$ = 7 per group) were randomly allocated to experimental groups to receive i.p. vehicle or different doses of WLB-73502 (1.25, 2.5 and 5 mg/kg), morphine (5, 10 and 20 mg/kg) or oxycodone (1.25, 2.5, 3.75 and 5 mg/kg). TFL was assessed 20 min after vehicle or drug administration.

#### 2.2.5. *Carrageenan-induced model of acute inflammatory pain*

The test was based on that previously described by Winter et al.[34]. The plantar surface of the right hind paw of the rats received a s.c. injection of carrageenan (200 μL of a 2% saline solution). To assess nociceptive responses, rats were placed on a metal grid in a

transparent methacrylate cylinder (200 mm diameter, 300 mm high, 3 mm thick) and then allowed to acclimate to their new environment 15 min before testing. Tactile allodynia was assessed 4 h after carrageenan injection by determination of the paw withdrawal threshold (PWT) to von Frey filaments stimulation (1−15 g) of the plantar surface of the hind paw. Each filament was applied 3 s until a paw withdrawal response was elicited. A single response indicated a positive response. Data were expressed as PWTs (g) of both the inflamed (ipsilateral, right) and non-inflamed (contralateral, left) hind paw, and as percentage of antinociception (antiallodynic effect) exerted by treatments on the ipsilateral hind paw respect to vehicle. A total of 112 animals were used to perform the experiments. No criteria for excluding animals were set and all animals in all experimental groups were included. Rats ($n$ = 9−10 per group) were randomly allocated to experimental groups to receive i.p. vehicle or different doses of WLB-73502 (1.25, 2.5 and 5 mg/kg), morphine (0.625, 2.5, 5, 10 and 15 mg/kg) or oxycodone (1.25, 2.5 and 5 mg/kg), and the PWT was evaluated 20 min after vehicle or drug administration.

#### 2.2.6. *MIA-induced model of osteoarthritis pain*

Osteoarthritis (OA) was induced by intraarticular injection of monosodium iodoacetate (MIA) in the right knee joint of rats, essentially as described by Dunham et al.[35]. Rats were briefly anesthetized with isoflurane (5% in 100% $O_2$) and maintained under anaesthesia (2% isoflurane in 100% $O_2$) by a facemask. The surgical area of the right knee was swabbed with chlorohexidine and alcohol, then a single injection of MIA (60 μL of a 40 mg/mL solution in 0.9% saline; *i.e.*, 2.4 mg/injection) was delivered using a 28-gauge needle into the joint space of the knee through the intra-patellar ligament, by a gentle flexion of the knee. After recovery, animals were returned to their home cage.

*2.2.6.1. Acute treatment.* A total of 102 animals were used to perform acute treatment experiments. No criteria for excluding animals were set and all animals in all experimental groups were included. Fourteen days after intraarticular MIA injection, rats ($n$ = 9−10 per group) were randomly allocated to experimental groups to receive i.p. vehicle or different doses of WLB-73502 (1.25, 2.5 and 5 mg/kg), morphine (2.5, 5 and 10 mg/kg) or oxycodone (1.25, 2.5, 5 and 10 mg/kg), and the PWT was evaluated 20 min after vehicle or drug administration. To assess nociceptive responses, PWT to von Frey filaments stimulation was assessed in the ipsilateral (right) and contralateral (left) hind paw, as previously described in carrageenan experiments. Data were expressed as pressure thresholds (g) of both ipsi- and contralateral hind paws, and as percentage of antinociception (antiallodynic effect) exerted by treatments on the ipsilateral hind paw respect to vehicle.

*2.2.6.2. Repeated (chronic) treatment long-term tolerance.* In another set of experiments (chronic treatment), a total of 50 animals ($n$ = 7−9 per group) were randomly allocated to experimental groups to receive repeated b.i.d. treatments with vehicle or different doses of WLB-73502 (0.5, 1.5, and 3 mg/kg), morphine (5 mg/kg) or oxycodone (2.5 mg/kg) through s.c. route. Animals that received vehicle or WLB-73502 were treated for 4 weeks and were evaluated for mechanical allodynia on Days 1, 3, 7, 10, 14, 21 and 28. Those administered with oxycodone or morphine were treated for 3 weeks and tested on Days 1, 3, 7, 10, 14 and 21. The Day 1 was the first day of the pharmacological treatment, *i.e.*, 14 days after MIA injection. No criteria for excluding animals were set and all animals in all experimental groups were included. To assess nociceptive responses, PWT to von Frey filaments stimulation was assessed in the ipsilateral (right) and contralateral (left) hind paw, both immediately before (pre-treatment) and 30 min after (post-treatment) morning vehicle or drug administration. Data were expressed as pressure thresholds (g) in both ipsi- and contralateral hind paws, both pre- and post-treatment, and as percentage of antinociception (antiallodynic effect) exerted by treatments (post-treatment effect) on the ipsilateral hind paw respect to vehicle.

#### 2.2.7. *Spared nerve injury model of neuropathic pain*

The spared nerve injury (SNI) procedure comprised an axotomy and ligation of the right tibial and common peroneal nerves leaving the sural nerve intact, essentially as described by Decosterd and Woolf[36]. Rats were briefly anesthetized with pentobarbital (50 mg/kg, i.p.) until lack of response to a toe pinch. Surgical area was swabbed with chlorohexidine and alcohol, the skin on the lateral surface of the thigh was incised and a section made directly through the biceps femoris muscle exposing the sciatic nerve and its three terminal branches: the sural, common peroneal and tibial nerves. The common peroneal and the tibial nerves were tight ligated with 5.0 silk and sectioned distal to the ligation, removing 2−4 mm of the distal nerve stump. Care was taken to avoid any contact with or stretching of the intact sural nerve. Muscle and skin were closed in two layers. After recovery, animals were returned to their home cage. To assess nociceptive responses, tactile allodynia was assessed by determination of the PWT (g) to von Frey filaments stimulation in the ipsilateral (right) and contralateral (left) hind paw, as described in carrageenan experiments, 14 days after surgery. Data were also expressed as percentage of antinociception (antiallodynic effect) exerted by treatments on the ipsilateral hind paw respect to vehicle. A total of 96 animals were used to perform the experiments. No criteria for excluding animals were set and all animals in all experimental groups were included. Rats ($n$ = 8 per group) were randomly allocated to experimental groups to receive i.p. vehicle or different doses of WLB-73502 (0.625, 1.25, 2.5 and 5 mg/kg), morphine (10, 15 and 20 mg/kg) or oxycodone (1.25, 2.5, 5 and 10 mg/kg), and the PWT was evaluated 20 min after vehicle or drug administration.

#### 2.2.8. *Intestinal transit inhibition (constipation)*

Intestinal transit was evaluated by identifying the leading front of an intragastrically administered marker (charcoal suspension) in the small intestine. A total of 64 rats were used to perform the experiments. No criteria for excluding animals were set and all animals in all experimental groups were included. Rats ($n$ = 8 per group) were fasted for 3−4 h and then given i.p. vehicle or different doses of WLB-73502 (2.5, 5, 10, or 20 mg/kg) or oxycodone (2.5, 5, or 10 mg/kg). Thirty min after vehicle or drug administration, 0.3 mL of a fresh 5% charcoal suspension in distilled water was administered by oral route using an intragastric probe, and rats were sacrificed 30 min later under $CO_2$ atmosphere saturation. The entire length of the small intestine was dissected free and removed from pylorus to ileocecal valve. The distance travelled by the charcoal meal, and the total length of the intestine were measured in cm. The percentage of the distance travelled by the charcoal meal in relation to the total length of the intestine was calculated.

*2.2.9. Whole body plethysmography (respiratory depression)*
Whole body plethysmography for unrestrained small animals controlled by Fine Pointe™ Software (Buxco, Data Sciences International; St. Paul, MN, USA) was used. Tidal volume (TV) and respiratory rate (RR) were assessed, and the minute volume (MV) was calculated. RR is the number of breaths taken per min. TV is the lung volume (mL); *i.e.*, the normal volume of air displaced between normal inspiration and expiration when extra effort is not applied. MV is the volume of gas inhaled or exhaled in 1 min (mL/min) and is the result of TV × RR.

A total of 64 rats were used to perform experiments. No criteria for excluding animals were set and all animals in all experimental groups were included. For acclimation, rats were placed into the plethysmography chambers 30 min prior to the test. Baseline respiratory parameters were measured continuously for 15 min before removing animals from the chambers for drug treatments. Rats ($n = 8$ per group) were randomly allocated to experimental groups to receive i.p. vehicle or different doses of WLB-73502 (1.25, 5, 10, and 20 mg/kg) or oxycodone (1.25, 5, and 10 mg/kg). After vehicle or drug administration, animals were returned to the plethysmography chambers and respiratory parameters were measured continuously for 30 min.

*2.2.10. Proemetic response in ferrets*
A total of 24 male ferrets were used to perform the experiments. No criteria for excluding animals were set and all animals in all experimental groups were included. Male ferrets ($n = 6$ per group) received a single i.p. administration of vehicle, WLB-73502 (0.5 and 1 mg/kg, i.p.) or morphine (0.5 mg/kg, s.c.) and were then observed continuously for 4 h for emesis and nausea-like behaviours quantification. During this period, nausea-like behaviour was evaluated by studying the occurrence of emesis (retching and vomiting; abdominal contractions without or with expulsion of part of the gastro-intestinal content, respectively) and typical emesis-related behaviours (licking, gagging, chewing, backward walking, head burying in cage shavings, wet dog shake, mouth clawing and prolonged typical ventral recumbency). For each animal, nausea-like global score was expressed as the sum of these different behaviours.

*2.2.11. Pharmacokinetics*
*2.2.11.1. Male Wistar rats treated with WLB-73502 at 3 mg/kg i.p. (single dose).* A total of 48 rats were used in this study (8 sampling points, 6 animals per sampling point). A single dose of 3 mg/kg of EST0073502.A was administered by i.p. route. Blood and brain sampling were performed at selected time points (5, 15 and 30 min, 1, 2, 4, 7 and 24 h). Briefly, after induction of anaesthesia (4% isoflurane in 100% $O_2$), the rat was maintained under anaesthesia (1%−2% isoflurane in 100% $O_2$) by a facemask and blood was collected by intracardiac puncture. After exsanguination, a cervical dislocation procedure was applied before brain extraction.

*2.2.11.2. Male Wistar rats from the MIA-induced OA pain study treated with WLB-73502 at 0.5, 1.5 and 3 mg/kg s.c (repeated b.i.d. dose for 28 days).* A total of 15 rats were used (same animals used in the MIA-induced OA pain study) and 3 treatment groups ($n = 5$/group) corresponding to the 3 dose levels (0.5, 1.5 and 3 mg/kg, s.c., b.i.d.) assayed. Blood samples were obtained from the caudal vein on Day 1 (first dose of the first day of administration) and at the end of the study on Day 28 (last dose of last day of administration) immediately after the pharmacodynamic (PD) evaluation (*i.e.*, 35−40 min after drug administration) in the MIA-induced model of OA pain.

*2.2.11.3. Male ferrets receiving single i.p. administration of WLB-73502 at 0.5 or 1 mg/kg (single dose).* A total of 4 ferrets ($n = 2$ per dose group) were implanted with an intra-arterial catheter the day before starting serial blood sampling. Briefly, after induction of anaesthesia (isoflurane 4% in 100% $O_2$), animals were maintained under isoflurane (1.5%−3% in 100% $O_2$) to allow catheterization. The catheter was introduced into the carotid artery, tunnelled subcutaneously and then fixed on the dorsal part of the neck. Special attention was paid to not damage the vagus nerve. At the end of the surgery, animals received a single s.c. administration of the anti-inflammatory carprofen (4 mg/kg). From each ferret, serial blood samples were collected by carotid catheterization at predose, 5, 15 and 30 min, 1, 2, 4, 7, and 24 h after i.p. administration of WLB-73502 at 0.5 or 1 mg/kg.

*2.2.11.4. Sample processing and analysis.* Blood samples (around 400 μL/sample) from ferrets and rats treated with WLB-73502 were collected into heparinized (ferrets and rat plasma/brain PK profiles) or $K_2$-EDTA (MIA-induced model of OA pain) anticoagulant tubes and centrifuged at 4 °C and 3700 × *g* for 10 min to obtain the plasma. Brains from rats treated with WLB-73502 were also obtained and homogenized with Dulbecco's phosphate buffered saline (DPBS; 1:5 *w/w* dilution). After protein precipitation of plasma or brain homogenates with acetonitrile, samples were processed and analysed to determine WLB-73502 concentrations by using an LC−MS/MS method, with a limit of quantification of 1 ng/mL for plasma and 2 ng/g for brain samples.

Standard pharmacokinetic (PK) parameters, such as area under the curve (AUC), peak plasma concentration ($C_{max}$), time to peak concentration ($T_{max}$) and terminal half-life ($t_{1/2}$), were determined by non-compartmental analysis of the plasma concentration−time curves (Phoenix v. 6.2.1.51; Pharsight, CA, USA).

*2.3. Ex vivo studies*

*2.3.1. Central receptor occupancy*
Central S1Rs and MORs occupancy by WLB-73502, morphine and oxycodone were investigated in rat brain (cortex and striatum) following their acute administration by *ex vivo* autoradiography. Two identically but separately processed studies were done, one (Study 1) including vehicle and WLB-73502, and the other (Study 2) including its own control (vehicle), morphine and oxycodone. A total of 25 ($n = 5$ per group) male Wistar rats (250−300 g) were used. No criteria for excluding animals were set and all animals in all experimental groups were included. Animals were i.p. administered vehicle (two groups, Study 1 and 2), WLB-73502 (3 mg/kg; one group, Study 1), morphine (10 mg/kg; one group, Study 2) or oxycodone (3 mg/kg; one group, Study 2) and terminated 15 (vehicle and WLB-73502; Study 1) or 30 (vehicle, morphine, and oxycodone; Study 2) min later by a rising concentration of $CO_2$ followed by cervical dislocation. Whole brains were removed and an anterior coronal block (cut at the level of the optic chiasm) containing the striatum was taken for autoradiography. The brain block was rapidly frozen in isopentane cooled to −20/−30 °C, coronal sections (20 μm) were obtained using a cryostat and thaw mounted onto silanised slides. Three adjacent sections were mounted onto each slide, two sections were used to

measure total binding and one section to measure non-specific binding. For each animal, 5 slides were prepared. The slides were stored at −20 °C until the day of assay. Slides were warmed to room temperature and incubated for 10 min with 50 mmol/L Tris−HCl, pH 7.4 (assay buffer) containing radioligands. Specific binding to MOR was determined using [$^3$H]-DAMGO (2.0 nmol/L) in the absence (total binding) or presence of naloxone (50 μmol/L, non-specific binding). Specific binding to S1R was determined using [$^3$H]-(+)-pentazocine (10 nmol/L) in the absence (total binding) or presence of haloperidol (10 μmol/L, non-specific binding). After incubation with radioligands, slides were washed for three consecutive 5 min periods in ice cold assay buffer. The slides were then rinsed briefly in ice cold distilled water to remove buffer salts and allowed to air dry. To make the slides conductive, copper foil tape was adhered to the free side of the microscope slide. The slides were placed in the $\beta$ imager (BioSpace, Nesles-la-Vallée, France) and the levels of bound radioactivity in the sections directly determined by counting the number of $\beta$ particles emerging using the M3 vision program (BioSpace). Data were collected from the delineated areas (cortex and striatum) of the brain sections over 16 h and expressed in counts per min per square millimeter (cpm/mm$^2$). The assay was performed on two separate occasions.

### 2.4. Data and statistical analysis

#### 2.4.1. In vitro

For the G protein pathway (cAMP determinations), the irreversible inactivation method, consisting of a collection of agonist curves in the absence or presence of increasing concentrations of the irreversible antagonist $\beta$-FNX, was used to estimate lg($\tau$) for each compound. For the $\beta$-arrestin pathway, the comparative method was used, assuming the maximal response and the slope parameter yielded by the full MOR agonist DAMGO to match the operational $E_m$ and $n$ parameters, respectively, and used as fixed values for the estimation of lg$\tau$ of partial agonists within the operational model[37]. All calculations were done using Graphpad Prism v. 9.0.0 software (San Diego, CA, USA).

#### 2.4.2. Ex vivo

For *ex vivo* autoradiography, the value for specific binding (cpm/mm$^2$) was generated by the subtraction of the mean non-specific binding from the mean total binding for each animal. Mean specific binding (cpm/mm$^2$) data were presented as a percentage of the vehicle treated control taken as 100%, Eq. (1).

$$\text{Receptor occupancy}\ (\%) = \left(\frac{\text{Specific binding}\ (\text{cpm}/\text{mm}^2)\ \text{vehicle} - \text{Specific binding}\ (\text{cpm}/\text{mm}^2)\ \text{treated}}{\text{Specific binding}\ (\text{cpm}/\text{mm}^2)\ \text{vehicle}}\right) \times 100 \quad (1)$$

#### 2.4.3. In vivo

The latency of tail withdrawal (s) was measured in the tail-flick test and the paw pressure threshold (g) evoking paw withdrawal in the paw pressure test. Sensitivity (hypersensitivity response) to mechanical stimulation with von Frey filaments (mechanical allodynia) was calculated as the difference in PWTs (g). The distance travelled by the charcoal meal *vs.* the total intestine length (cm) was measured to evaluate intestinal transit (IT) and the percentage of IT was calculated. RR (breaths/min) and TV (mL) were measured in the plethysmograph and MV (mL/min) calculated. The percentage (%) of effect was determined by the following Eqs. (2)−(6):

$$\text{Tail-flick}: \text{Antinociceptive effect}\ (\%) = \left(\frac{\text{Drug latency} - \text{Vehicle latency}}{\text{Cut-off latency} - \text{Vehicle latency}}\right) \times 100 \quad (2)$$

$$\text{Paw pressure: Antinociceptive effect}\ (\%) = \left(\frac{\text{Drug pressure threshold} - \text{Vehicle pressure threshold}}{\text{Cut-off pressure threshold} - \text{Vehicle pressure threshold}}\right) \times 100 \quad (3)$$

$$\text{Mechanical sensitivity: Antiallodynic effect}\ (\%) = \left(\frac{\text{Drug PWT (Ipsi)} - \text{Vehicle PWT (Ipsi)}}{\text{Contralateral PWT} - \text{Vehicle PWT (Ipsi)}}\right) \times 100 \quad (4)$$

$$\text{Intestinal transit inhibition: IT inhibition}\ (\%) = \left(\frac{\text{Drug IT} - \text{Vehicle IT}}{\text{Vehicle IT}}\right) \times 100 \quad (5)$$

$$\text{Respiratory depression (minute volume): MV inhibition}\ (\%) = \left(\frac{\text{Drug MV} - \text{Vehicle MV}}{\text{Vehicle MV}}\right) \times 100 \quad (6)$$

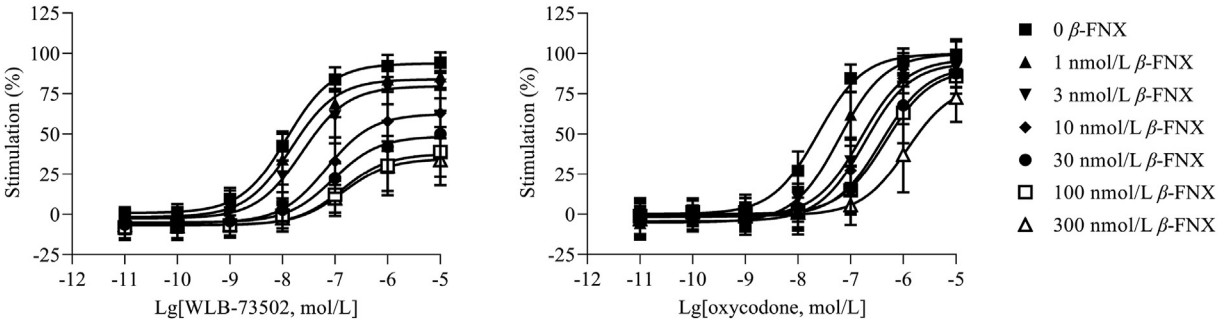


**Figure 1** MOR agonist-mediated inhibition of forskolin-stimulated cAMP production. The concentration−response curves of WLB-73502 and oxycodone were determined relative to DAMGO (1 μmol/L) as reference full agonist in this assay, in the absence (0) and presence (1, 3, 10, 30, 100, 300 nmol/L) of the irreversible MOR antagonist β-FNX. $n = 5$ independent experiments. In each experiment, data points (mean ± SEM) were obtained from duplicates.

Dose−response curves were generated and $ED_{50}$ values (means ± standard error) were calculated by curve fitting to a four-parameter logistic equation (sigmoidal dose−response curve, variable slope) by means of least squares non-linear fitting using GraphPad Prism v. 9.0.0 software. The $ED_{50}$ was defined as the dose that produced 50% of the maximum possible effect. In the rest of experiments, values are given as mean ± standard error of the mean (SEM). Statistical significance was estimated with one-way ANOVA followed by Bonferroni's multiple comparisons *post hoc* test. The level of significance was set at $P < 0.05$. Statistical analyses were done using GraphPad Prism v. 9.0.0 software.

## 3. Results

### 3.1. *In vitro functional profile*

#### 3.1.1. *MOR functionality*

WLB-73502 induces negative coupling of MOR to adenylyl cyclase and thus behaves as MOR agonist at the cAMP-dependent pathway, but accurate determination of its functional nature (*i.e.*, full *vs.* partial agonism) cannot be established in cell lines over-expressing MOR, with a high receptor reserve[37,38]. Accordingly, the efficacy of WLB-73502 was evaluated by a cAMP determination assay on CHO-K1 cells stably expressing the human MOR, following partial receptor inactivation in presence of increasing concentrations of the irreversible MOR antagonist β-FNX (Fig. 1). MOR agonist inhibition of forskolin-stimulated cAMP production in presence of β-FNX revealed a partial agonist activity of WLB-73502 (∼30% maximal efficacy in presence of the highest concentrations of β-FNX). The maximal efficacy of the full MOR agonist oxycodone was much less affected by β-FNX. To accurately quantify and compare, concentration−response curves were subjected to operational analysis and $\tau$ values calculated (Supporting Information Table S1). This analysis revealed a statistically significant partial agonist activity for WLB-73502 ($\lg\tau = 1.58$) as compared to classical full opioid agonists such as morphine ($\lg\tau = 2.11$), oxycodone ($\lg\tau = 2.18$) or fentanyl ($\lg\tau = 2.23$).

A complementation assay was used to assess β-arrestin-2 recruitment elicited by MOR agonist ligands. Concentration−response curves (Fig. 2A) were subjected to operational analysis and $\tau$ values calculated (Table S1). WLB-73502 had no effect in this signalling pathway and thus the operational $\lg\tau$ parameter could not be determined. Traditional opioids, like morphine ($\lg\tau = -0.19$), oxycodone ($\lg\tau = -0.28$) or fentanyl ($\lg\tau = 0.31$) recruited the β-arrestin signalling pathway to some extent, as published previously[37]. Accordingly, the maximal effect ($E_{max}$) for β-arrestin-2 recruitment elicited of WLB-73502 was significantly different from the $E_{max}$ of the other MOR agonists assayed (morphine, oxycodone and fentanyl) (Table S1).

#### 3.1.2. *S1R functionality*

Phenytoin (diphenylhydantoin, DPH) is a positive allosteric S1R modulator that shifts S1R agonists to significant higher binding affinities ($K_i$ ratios without DPH *vs.* with DPH > 1), while no shift or a very little shift to lower affinity values ($K_i$ ratios without DPH *vs.* with DPH ≤ 1) occurs with antagonists[29]. WLB-73502 produced a small, non-significant shift to lower affinity values when incubated with DPH ($K_i$ without DPH/$K_i$ with DPH = 0.9), which indicated antagonist properties at the S1R (Fig. 3). A similar small non-significant shift to the right was also found for the reference S1R antagonist haloperidol, whereas DPH significantly shifted the curve of the reference S1R agonist dextromethorphan to higher affinity ($K_i$ without DPH/$K_i$ with DPH = 9.0).

### 3.2. *Antinociceptive effect after single administration in rat models of pain*

The effect of single i.p. administration of WLB-73502, morphine and oxycodone on mechanical (paw pressure test) and thermal (tail-flick test) sensitivity, and on mechanical hypersensitivity (mechanical allodynia) following somatic inflammatory (carrageenan paw injection), osteoarthritis (MIA knee injection) and neuropathic (SNI) pain induction was evaluated (Fig. 4 and Table 1).

#### 3.2.1. *Paw pressure test*

Single administration by i.p. route of WLB-73502 (1.25, 2.5, and 5 mg/kg), morphine (5, 7.5, 10, and 20 mg/kg) or oxycodone (1.25, 2.5, and 3.75 mg/kg) dose-dependently inhibited paw pressure-induced mechanical nociception (Fig. 4A, Supporting Information Fig. S1A and S1B), reaching a maximal efficacy ≥80%. WLB-73502 was 3-fold more potent than morphine ($P < 0.05$) and had a potency similar to oxycodone (Table 1).

#### 3.2.2. *Tail flick test*

Single systemic i.p. administration of WLB-73502 (1.25, 2.5, and 5 mg/kg), morphine (5, 10, and 20 mg/kg) and oxycodone (1.25,

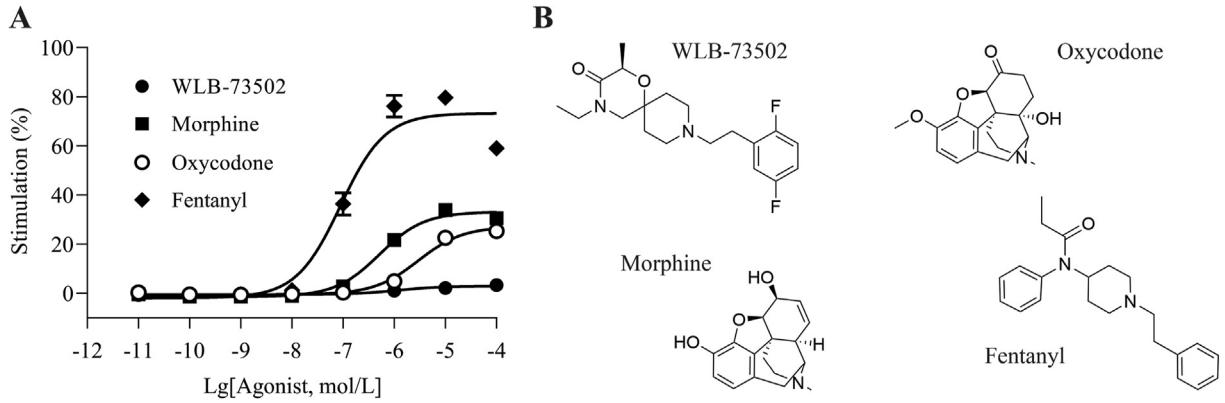


**Figure 2** MOR agonist-mediated $\beta$-arrestin recruitment (A) and molecular structure of assayed ligands (B). The concentration−response curves of WLB-73502, morphine, oxycodone and fentanyl were determined relative to the concentration−response curve of DAMGO as reference full agonist in this assay. $n = 5$ except for fentanyl ($n = 3$) independent experiments. In each experiment, data points (mean ± SEM) were obtained from quadruplicates.

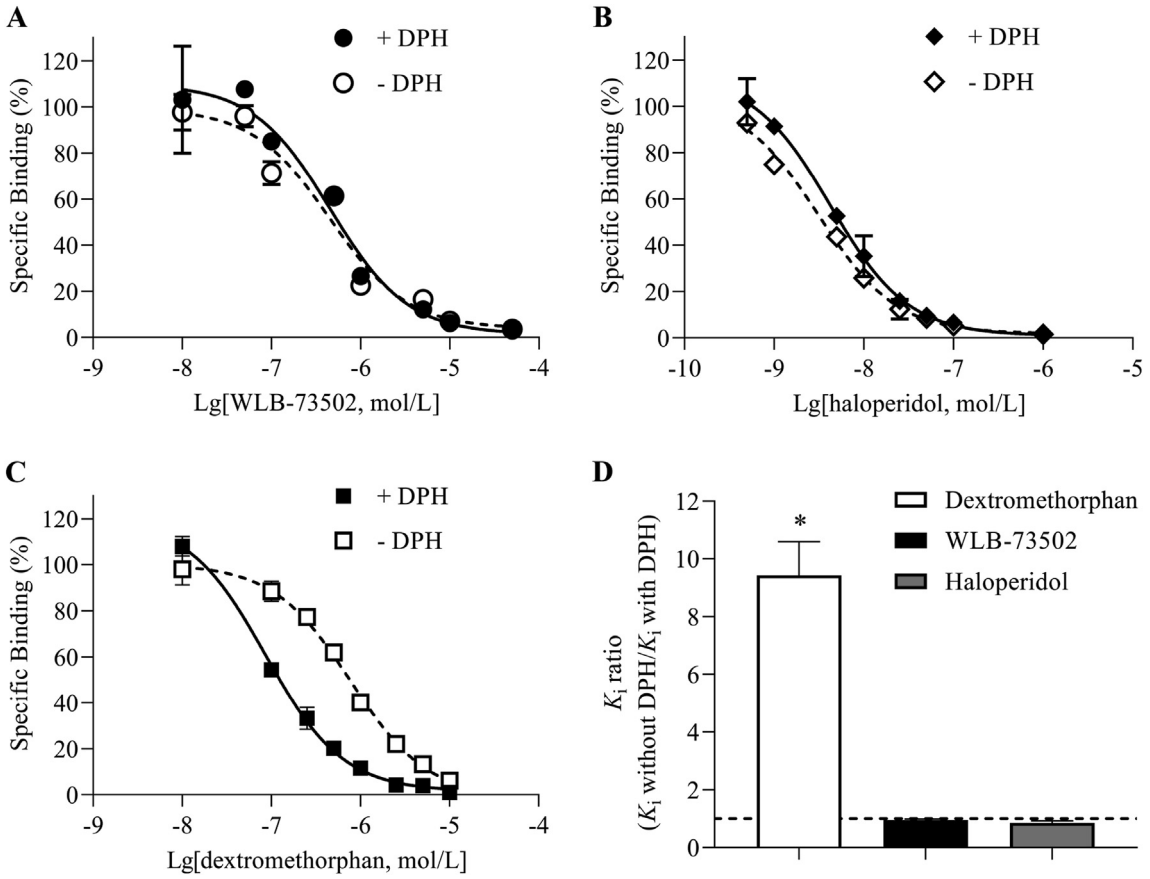


**Figure 3** DPH modulation of S1R binding. Inhibition by WLB-73502 (A), haloperidol (B) and dextromethorphan (C) of [$^3$H](+)-pentazocine binding to guinea pig brain membranes in the absence (open symbols) or presence (closed symbols) of 1 mmol/L DPH. Ratios of the $K_i$ value in the absence and presence of 1 mmol/L DPH for WLB73502, haloperidol and dextromethorphan (D). $n = 5$ independent experiments. In each experiment, data points (mean ± SEM) were obtained from duplicates. *$P < 0.05$ *vs.* ratio = 1 (one-way ANOVA followed by Bonferroni's *post hoc* test).

2.5, 3.75, and 5 mg/kg) dose-dependently inhibited acute thermal nociception (Fig. 4B, Fig. S1C and S1D), with efficacies reaching a maximal effect ≥95%. WLB-73502 showed 4-fold more potency than morphine ($P < 0.05$) and similar potency to oxycodone (Table 1).

*3.2.3. Carrageenan-induced model of acute inflammatory pain*

A significant decrease in the withdrawal thresholds to von Frey stimulation (*i.e.*, mechanical allodynia) was observed in the ipsilateral paw 4 h after intraplantar carrageenan injection. Single i.p. administration of WLB-73502 (1.25, 2.5, and 5 mg/kg), morphine

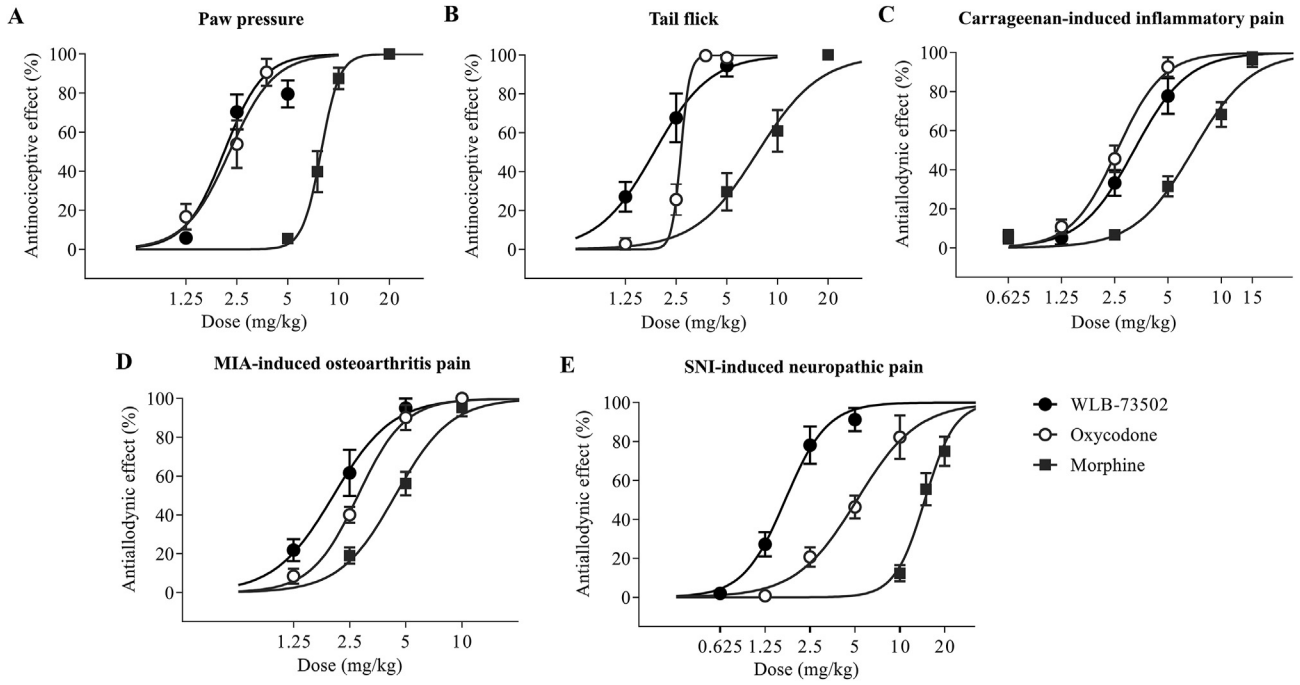


**Figure 4** Acute antinociceptive/antiallodynic effect. Dose−response curves of the effect of single administration of WLB-73502, morphine or oxycodone on mechanical nociception in the paw pressure test (A), on thermal nociception in the tail flick test (B), and on mechanical allodynia in carrageenan-induced inflammatory (C), MIA-induced OA (D) and SNI-induced neuropathic (E) pain models in male Wistar rats. $n = 7$ (paw pressure and tail flick), $n = 9$−10 (carrageenan and MIA) and $n = 8$ (SNI) per treatment group. Values are expressed as percentage of effect. Points and vertical lines represent the mean ± SEM.

**Table 1** $ED_{50}$ values of the antinociceptive/antiallodynic effect of WLB-73502, oxycodone and morphine on acute mechanical (paw pressure) and thermal (tail-flick) nociception, and on mechanical allodynia in pain models of different aetiology following single i.p. administration in male Wistar rats.

| Animal pain model | $ED_{50}$ (mg/kg)[a] | | |
|---|---|---|---|
| | WLB-73502 | Oxycodone | Morphine |
| Mechanical nociception | | | |
| Paw pressure | 2.11 ± 0.18 | 2.27 ± 0.22 | 7.88 ± 0.24* |
| Thermal nociception | | | |
| Tail-flick | 1.85 ± 0.22 | 2.67 ± 0.46 | 7.63 ± 0.96* |
| Inflammatory pain − mechanical allodynia | | | |
| Carrageenan-induced inflammation | 3.11 ± 0.34 | 2.68 ± 0.15 | 6.94 ± 0.42* |
| Osteoarthritis pain − mechanical allodynia | | | |
| MIA-induced osteoarthritis | 2.05 ± 0.20 | 2.77 ± 0.13 | 4.39 ± 0.28* |
| Neuropathic pain − mechanical allodynia | | | |
| SNI-induced neuropathy | 1.71 ± 0.14 | 5.17 ± 0.44* | 14.72 ± 0.73* |

[a]Data are mean ± SEM; $n = 7$ (paw pressure and tail flick), $n = 9$−10 (carrageenan and MIA) and $n = 8$ (SNI) per treatment group. *$P < 0.05$ *vs.* WLB-73502 (one-way ANOVA followed by Bonferroni's *post hoc* test).

(0.625, 2.5, 5, 10, and 15 mg/kg) or oxycodone (1.25, 2.5, and 5 mg/kg) dose-dependently reversed carrageenan-induced mechanical allodynia in the ipsilateral paw (Fig. 4C and Supporting Information Fig. S2). Maximal effect was ≥80% for all treatments. WLB-73502 was 2-fold more potent than morphine ($P < 0.05$) and had similar potency to oxycodone (Table 1). Mechanical allodynia did not develop in the contralateral paw and treatments did not exert significant effects on the contralateral paw (Fig. S2).

*3.2.4. MIA-induced model of OA pain*

A significant decrease in the withdrawal thresholds to von Frey stimulation was observed in the ipsilateral paw 14 days after MIA injection into the knee joint. WLB-73502 (1.25, 2.5, and 5 mg/kg), morphine (2.5, 5, and 10 mg/kg) or oxycodone (1.25, 2.5, 5, and 10 mg/kg) dose-dependently reversed mechanical allodynia in the ipsilateral paw reaching a maximal effect ≥95% (Fig. 4D and Supporting Information Fig. S3). WLB-73502 showed 2-fold more potency than morphine ($P < 0.05$) and similar potency to

**Table 2** PK parameters of WLB-73502 in plasma and brain following i.p. administration of 3 mg/kg to adult male Wistar rats.

| Compound | Matrix | $t_{1/2}$ (h) | $T_{max}$ (h) | $C_{max}$ [a] | $AUC_{0-\infty}$ [a] | Brain-to-plasma ratio (AUC brain/AUC plasma) |
|---|---|---|---|---|---|---|
| WLB-73502 | Plasma | 0.30 | 0.08 | 441 ± 73 (ng/mL) | 136 ± 15 (ng·h/mL) | 2.57 |
| | Brain | 0.34 | 0.08 | 982 ± 191 (ng/g) | 350 ± 40 (ng·h/g) | |

[a]Data are mean ± SEM; $n = 6$ (8 sampling points, 6 animals per sampling point).

oxycodone (Table 1). Mechanical allodynia did not develop in the contralateral paw and treatments did not exert significant effects on the contralateral paw (Fig. S3).

#### 3.2.5. *SNI model of neuropathic pain*

A significant decrease in the withdrawal thresholds to von Frey stimulation was observed in the ipsilateral paw 14 days after SNI surgery. Administration of WLB-73502 (0.625, 1.25, 2.5, and 5 mg/kg), morphine (10, 15, and 20 mg/kg) or oxycodone (1.25, 2.5, 5, and 10 mg/kg) dose-dependently reversed mechanical allodynia in the ipsilateral paw reaching a maximal effect of 91.2 ± 5.9%, 82.2 ± 11.1% and 74.9 ± 7.5% respectively (Fig. 4E and Supporting Information Fig. S4). WLB-73502 was 8- and 3-fold more potent than morphine and oxycodone, respectively ($P < 0.05$) (Table 1). It is worth noting that morphine and oxycodone required higher doses to exert antinociception in the SNI-induced neuropathic pain model than in the other pain models, whereas WLB-73502 showed a similar potency in all of them (Table 1). Mechanical allodynia did not develop in the contralateral paw and treatments did not exert significant effects on the contralateral paw (Fig. S4).

### 3.3. *Brain penetration, receptor occupancy and PK/PD relationship after single administration*

#### 3.3.1. *Plasma and brain pharmacokinetics*

Drug levels were analysed by LC−MS/MS in plasma and brain samples following single i.p. administration of WLB-73502 at 3 mg/kg (a dose that produces 45%−85% antinociceptive effect, depending on the test) in male Wistar rats. Standard PK parameters were determined by non-compartmental analysis of the concentration−time curves (Table 2). Plasma $C_{max}$ following i.p. administration was reached very quickly ($T_{max} = 5$ min; first sampling time) and the compound was rapidly eliminated ($t_{1/2} = 20$ min). The compound crossed the blood−brain barrier (BBB). Indeed, brain kinetics was parallel to plasma kinetics, with high brain penetration: both the peak ($C_{max}$) and extent (AUC) of WLB-73502 exposure were higher in brain than in plasma (brain-to-plasma partition coefficient = 2.6).

#### 3.3.2. *Brain receptor occupancy*

The occupancy of MOR and S1R following i.p. drug administration was studied by *ex vivo* autoradiography in brain sections from male Wistar rat (Supporting Information Fig. S5 and Table S2).

Robust binding of [$^3$H]-DAMGO (MOR radioligand) and [$^3$H]-(+)-pentazocine (S1R radioligand) on brain sections was found in cortex and striatum of vehicle-treated rats, according to the reported distribution of MOR[39] and S1R[40] in rat brain (Fig. S5). Both cortex and striatum exhibited high levels of specific binding, as defined by incubations in presence of 50 μmol/L naloxone and 10 μmol/L haloperidol.

Administration of WLB-73502 at 3 mg/kg i.p. significantly inhibited [$^3$H]-DAMGO specific binding in rat brain cortex (51% occupancy) and striatum (50% occupancy) 15 min after dosing when compared to vehicle-treated controls. Similarly, WLB-73502 at 3 mg/kg i.p. significantly inhibited [$^3$H]-(+)-pentazocine specific binding in cortex (57% occupancy) and striatum (63% occupancy) 15 min after dosing when compared to vehicle-treated controls (Table S2).

A significant inhibition of [$^3$H]-DAMGO specific binding by morphine at 10 mg/kg i.p. was observed in rat cortex (51% occupancy) and striatum (52% occupancy) 30 min after dosing when compared to vehicle-treated controls. Oxycodone at 3 mg/kg i.p. also significantly inhibited [$^3$H]-DAMGO specific binding in rat cortex (40% occupancy) and striatum (44% occupancy) when compared to vehicle-treated controls. In contrast, neither morphine nor oxycodone had a significant effect on [$^3$H]-(+)-pentazocine specific binding in rat cortex and striatum (Table S2).

#### 3.3.3. *PK/PD relationship*

A preliminary PK/PD relationship was established from the brain exposure and the antinociceptive response at a single point following single i.p. administration of WLB-73502 at 3 mg/kg, the dose and route of administration used in brain receptor occupancy studies.

Antinociceptive efficacy, calculated from the dose−response curves (Fig. 4) in the different models 20 min after administration of WLB-73502 at 3 mg/kg i.p., corresponds to 45%−85% (average 75%), depending on the test. Experimental processing for receptor occupancy was initiated 15 min after compound administration at 3 mg/kg i.p. and occupancies were 50%−51% for MOR and 57%−63% for S1R, depending on the brain region (Table S2). Finally, experimental brain concentrations quantified at 15 and 30 min after i.p. administration of WLB-73502 at 3 mg/kg (PK parameters summarized in Table 2) were 127.6−236.5 ng/g, that correspond to a brain concentration of 362.0−671.1 nmol/kg. Considering the brain tissue binding of WLB-73502 in the rat (49.9%)[41], the free, unbound fraction corresponds to 181.4−336.2 nmol/kg. As a reference, the binding to human MOR and S1R is 64 and 118 nmol/L, respectively[28]. Table 3 summarizes the above *in vitro* pharmacological, *ex vivo* autoradiography and *in vivo* PK and PD data. There was a consistency between brain exposure, MOR and S1R affinities, brain MOR and S1R occupancy, and antinociceptive efficacy, although efficacy was a bit higher than expected based on a direct translation of receptor occupancies.

### 3.4. *Tolerance to the antinociceptive effect*

#### 3.4.1. *MIA-induced OA model (pharmacodynamics)*

WLB-73502 (0.5, 1.5, and 3 mg/kg), oxycodone (2.5 mg/kg) or morphine (5 mg/kg) were administered during 28 (WLB-73502) or 21 days (oxycodone and morphine) by s.c. instead of i.p. route

**Table 3** PK/PD relationship after single i.p. administration of WLB-73502 at 3 mg/kg to male Wistar rats.

| Antinociceptive efficacy (range in the different pain model) | Brain receptor occupancy (cortex-striatum) | Total brain concentration (30−15 min) | Unbound brain concentration (30−15 min) | *In vitro* binding affinity ($K_i$) |
|---|---|---|---|---|
| 45%−85% | 50%−51% (MOR)<br>57%−63% (S1R) | 362.0−671.1 nmol/kg | 181.4−336.2 nmol/kg | 64 nmol/L (MOR)<br>118 nmol/L (S1R) |

Antinociceptive efficacy obtained from dose−responses curves in the different pain models (paw pressure, tail-flick, and carrageenan-, MIA- and SNI-induced pain) 20 min after compound administration. Experimental processing for brain MOR and S1R occupancy was initiated 15 min after compound administration. Brain concentrations obtained from experimental quantifications at 15 and 30 min after compound administration. Unbound, free fraction was calculated subtracting the bound fraction (rat brain tissue binding: 49.9%)[41]. Binding affinities ($K_i$) *in vitro* correspond to human MOR and S1R[28]. $n = 7$ (paw pressure and tail flick), $n = 9-10$ (carrageenan and MIA) and $n = 8$ (SNI) for antinociceptive efficacy; $n = 5$ for receptor occupancy; and $n = 6$ for brain concentration studies.

to diminish first-pass liver metabolism and b.i.d. to favour around-the-clock drug exposure. Drug treatments started 14 days after intraarticular MIA injection (when mechanical allodynia had fully developed) and the effect on MIA-induced mechanical allodynia was evaluated every 3−4 days, 30 min after daily administrations. Systemic b.i.d. administration of WLB-73502 induced a dose-dependent reduction of MIA-induced mechanical hypersensitivity in the ipsilateral paw. The effect of WLB-73502 remained unchanged throughout the treatment period, with a tendency to increase efficacy overtime (significant by the end of

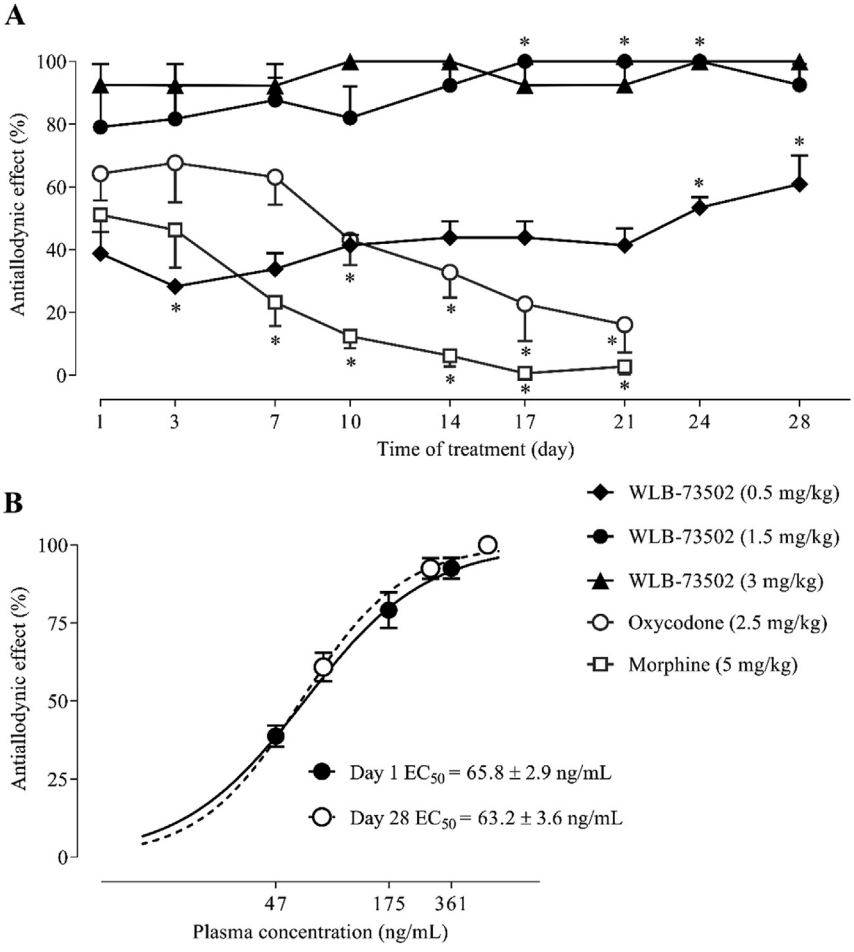


**Figure 5** Antiallodynic effect on MIA-induced mechanical allodynia following subchronic administration. Time−course effect of WLB-73502, morphine or oxycodone on mechanical allodynia after repeated b.i.d. s.c. administration starting 14 days after intraarticular MIA injection in male Wistar rats (A). Plasma concentration−response curves on Day 1 (single administration) and after 28 days of b.i.d. s.c. administration of WLB-73502 (B). Points and vertical lines represent the mean ± SEM. $n = 7-9$ (A) and $n = 5$ (B, from animals used in A) per treatment group. *$P < 0.05$ *vs.* corresponding Day 1 (one-way ANOVA followed by Bonferroni's *post hoc* test).

treatment when compared with Day 1 at 0.5 and 1.5 mg/kg doses exerting submaximal effects), thus suggesting absence of tolerance to its analgesic effect after 4 weeks of repeated administration (Fig. 5A and Supporting Information Fig. S6). Oxycodone (2.5 mg/kg) and morphine (5 mg/kg) also reduced mechanical hypersensitivity, but their antinociceptive effect progressively diminished throughout the treatment period (*i.e.*, pharmacodynamic tolerance developed) ($P < 0.05$), the effect being almost completely lost after 3 weeks of treatment (Fig. 5A and Fig. S6). Mechanical allodynia did not develop in the contralateral paw and treatments did not exert significant effects on the contralateral paw. No effect was observed either before daily drug administration (pre-treatment) or following vehicle-treatment, supporting that mechanical allodynia remained stable throughout the treatment period and that effects were indeed attributable to drug treatments (Fig. S6).

#### 3.4.2. *MIA-induced OA model (pharmacokinetics)*

Plasma samples from rats treated with WLB-73502 were obtained on Days 1 (first day of administration) and 28 (last day of administration) immediately after the PD evaluation (*i.e.*, 35−40 min after drug administration) in the MIA-induced model of OA knee pain (same animals used in the PD study) to explore the possibility that progressive drug accumulation could mask the development of tolerance. The mean plasma concentration of WLB-73502 was 361 ± 24.7 ng/mL on Day 1 and 550.6 ± 33.8 ng/mL on Day 28 when the compound was administered at 3 mg/kg. When administered at the dose of 0.5 mg/kg the values ranged 47.3 ± 3.8 ng/mL on Day 1−82 ± 3.2 ng/mL on Day 28; and 174.9 ± 7.4 ng/mL on Day 1−283.7 ± 10.4 ng/mL on Day 28 when administered at 1.5 mg/kg (Supporting Information Table S3). Accordingly, there was drug accumulation (factor 1.5−1.7) following repeated b.i.d. s.c. treatment for 28 days based on the comparison of levels attained at a single point after PD evaluation the first and last day of administration. Efficacy on MIA-induced mechanical allodynia was also superior on Day 28 compared to Day 1 (factor 1.2−1.6), particularly at the lower doses (0.5 and 1.5 mg/kg) ($P < 0.05$) exerting submaximal effects (Fig. 5A and Fig. S6). To find out if tolerance really did develop, plasma concentration−effect curves on Day 1 and Day 28 were done and mean concentrations providing half of maximum analgesia ($EC_{50}$s) calculated (Fig. 5B). There were no differences between Days 1 and 28 (Day 1 $EC_{50}$ = 65.8 ± 3 ng/mL; Day 28 $EC_{50}$ = 63.2 ± 4 ng/mL), which demonstrated that efficacy of WLB-73502 was maintained over time, with neither increase nor decrease, and that the absence of pharmacodynamic tolerance was not due to a pharmacokinetic effect.

### 3.5. *Gastrointestinal transit (constipation)*

The effect of WLB-73502 (2.5, 5, 10, and 20 mg/kg) and oxycodone (2.5, 5, and 10 mg/kg) on gastrointestinal motility was evaluated in male Wistar rats. Drug was i.p. administered 30 min before *p.o.* administration of the charcoal suspension, and passage of charcoal through the intestine was measured 30 min later. Treatments induced a significant dose-dependent intestinal transit inhibition as shown by a reduced percentage of the distance travelled by the charcoal meal *vs.* the total length of the small intestine (Fig. 6A). WLB-73502 did not significantly inhibit the intestinal transit at 2.5 and 5 mg/kg, and induced partial intestinal transit inhibition at 10 mg/kg (19%) and 20 mg/kg (59%). Oxycodone had no effect at 2.5 mg/kg but it reduced intestinal transit by 72% at 5 mg/kg and produced close to full blockade of intestinal transit (93% of inhibition) at 10 mg/kg. It is worth noting that, contrary to oxycodone, WLB-73502 elicited remarkable/maximal antinociceptive effect at doses devoid of significant effect on intestinal transit (Fig. 6A).

### 3.6. *Whole body plethysmography (respiratory depression)*

The effect of WLB-73502 (1.25, 5, 10, and 20 mg/kg) and oxycodone (1.25, 5, and 10 mg/kg) on respiratory function in male Wistar rats was evaluated by whole-body plethysmography. Basal respiratory parameters were recorded continuously for 15 min and the effect of drugs was then evaluated along 30 min, starting immediately after i.p. compound administration when animals returned to the plethysmography chambers. WLB-73502 did not

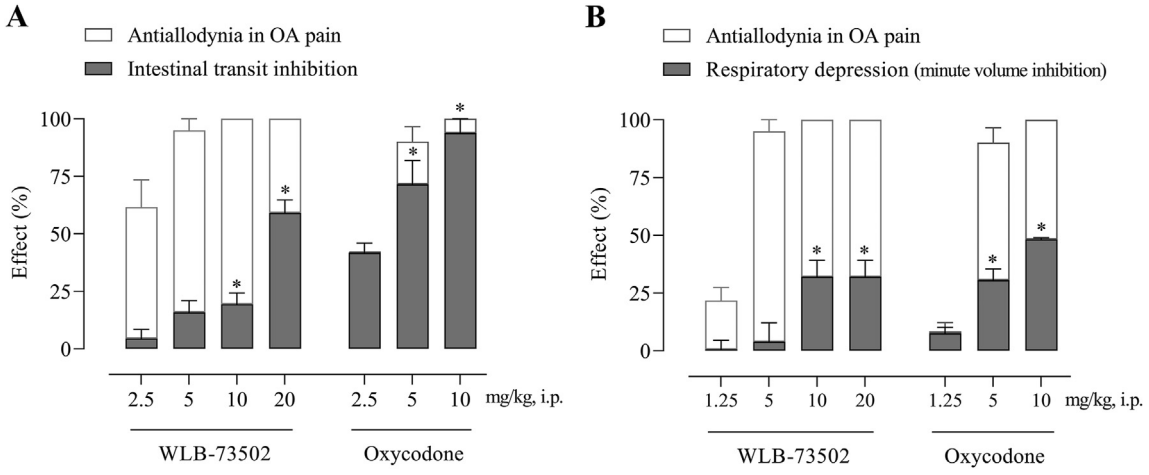


**Figure 6** Dose−response effect of single administration of WLB-73502 and oxycodone on intestinal transit measured in the charcoal test (A) and respiratory function measured as minute volume (B) in male Wistar rats. Values in grey bars are mean ± SEM percentage of effect (A, intestinal transit inhibition; B, respiratory depression) *vs.* vehicle. For comparison, the percentage of antiallodynic effect on OA pain (white bars) achieved at the same doses is also shown. $n = 8$ per treatment group. *$P < 0.05$ *vs.* vehicle (one-way ANOVA followed by Bonferroni's *post hoc* test).

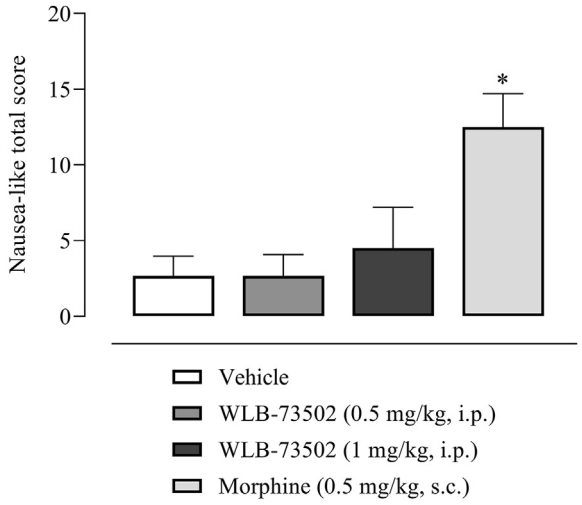


**Figure 7** Effect of single administration of WLB-73502 or morphine on emetic response in male ferrets. Values in bars are mean ± SEM. nausea-like total scores (sum of retching, vomiting, and other nausea-related behaviours including licking, gagging, chewing, backward walking, head burying in cage shavings, wet dog shake, mouth clawing and prolonged typical ventral recumbency) recorded for 4 h following compound administration. $n = 6$ per treatment group. $^*P < 0.05$ *vs.* vehicle group (one-way ANOVA followed by Bonferroni's *post hoc* test).

significantly change MV when administered in the analgesic dose range (1.25 and 5 mg/kg), but it reduced MV at 10 and 20 mg/kg. The inhibitory effect reached a plateau of ~30% reduction, with no differences between the 10 and 20 mg/kg doses. Oxycodone did not significantly modify MV when administered at 1.25 mg/kg, but it inhibited MV by 30% and 50% when administered at 5 and 10 mg/kg, respectively. Note that, contrary to oxycodone, WLB-73502 elicited antinociceptive effect at doses devoid of significant effect on respiration (Fig. 6B).

### 3.7. *Emesis (nausea and vomiting)*

#### 3.7.1. *Pharmacodynamics*

The study was done in ferrets as rats lack the emetic reflex and predictive value of pica behaviour in rodents remains questionable[42]. Male ferrets received a single i.p. administration of WLB-73502 (0.5 and 1 mg/kg, i.p.) or morphine (0.5 mg/kg, s.c.) and were then observed continuously for 4 h for emesis and nausea-like behaviours quantification. Emetic responses (retching and vomiting) and other typical nausea-like-related behaviours were summed up to get a nausea-like global score (Fig. 7). Control animals administered with vehicle did not show any emetic response, neither retching nor vomiting episodes, and the nausea-like global score was ~2. WLB-73502 did not induce any emetic response at 0.5 mg/kg or 1 mg/kg i.p., and scored ~2 and ~4, respectively. In contrast, morphine (0.5 mg/kg, s.c.) induced emetic responses during the 4 h period after its administration (2.17 ± 0.60 retches and 1.17 ± 0.65 vomits) and scored ~12 (Fig. 7).

#### 3.7.2. *Pharmacokinetics*

We estimated the PK profile of WLB-73502 in plasma samples from male ferrets to verify if tested doses (0.5 and 1 mg/kg, i.p) provided the plasma exposure needed to elicit analgesia in rat pain models. Plasma exposure after single i.p. administration of WLB-73502 was higher in ferrets (Table S4) than in rats (Table 3). Both $C_{max}$ (620 ± 98 ng/mL) and $AUC_{0-\infty}$ (2463 ± 625 ng·h/mL) in ferrets at 1 mg/kg exceeded by far values obtained in rats administered with the active 3 mg/kg dose ($C_{max}$ = 441 ± 73 ng/mL, $AUC_{0-\infty}$ = 136 ± 15 ng·h/mL), suggesting that analgesia by WLB-73502 would be achievable in ferrets without accompanying emesis.

## 4. Discussion

The current study investigated the intrinsic activity on MOR and S1R, brain exposure, target engagement and ultimately the benefit-risk (efficacy-safety) balance of WLB-73502 in comparison with morphine and oxycodone.

WLB-73502 binds to human MOR ($K_i$ = 64 nmol/L) and S1R ($K_i$ = 118 nmol/L) but it is selective against a panel of more than 180 targets including receptors, transporters, ion channels and enzymes[28]. The activation of MOR induces distinct intracellular signalling pathways that can be differentially stimulated, including i) activation of the $G\alpha_i$ subunit, which inhibits adenylyl cyclase and reduces cAMP intracellular levels; and ii) recruitment of β-arrestins, scaffolding proteins that hinder the G-protein coupling of agonist-activated GPCRs, ultimately resulting in receptor desensitization[43]. Biased opioid agonists showing a preference for activating the G-protein *versus* the β-arrestin pathway (*i.e.*, G-protein biased MOR agonists) were proposed to be safer opioid analgesics[11,44]. WLB-73502 behaved as a partial agonist at the MOR G-protein pathway and was inactive in the β-arrestin-2 signalling pathway. This is in contrast with conventional opioids such as morphine, oxycodone or fentanyl, that behaved as full agonists at the MOR G-protein pathway and recruited β-arrestin signalling to some extent. Responses and operational τ values were lower for all MOR agonists in β-arrestin than in cAMP determinations. Indeed, reduced intrinsic efficacy, ceiling effects and distortions by analysis of amplified (G-protein) *versus* linear (arrestin) signalling mechanisms may lead to bias overestimation, the weaker the G-protein partial agonism is the greater the apparent bias[6,45,46]. Despite these constrains, biased agonism favouring G protein signalling was supported for some MOR partial agonists[47]. Is WLB-73502 a G-protein-biased MOR agonist? Bias is suggested, but it can neither be established nor ruled out based on the inactivity of WLB-73502 in the β-arrestin recruitment assay. Independent on bias, WLB-73502 had lower intrinsic efficacy than oxycodone, morphine and fentanyl at both G-protein and β-arrestin pathways. This confirms its partial MOR agonist nature, which together with its bispecific ability to block S1R may explain its safety superiority.

The antagonistic activity on S1R is a key differential feature of WLB-73502. The S1R, a non-opioid receptor, was first identified as a tonically active antiopioid system by Chien and Pasternak[48], who reported that S1R agonists lower and S1R antagonists enhance opioid analgesia[22,48]. They also first noticed that S1R functionally regulate opioid analgesia without affecting other opioid-related effects, particularly morphine's effects on gastrointestinal transit or lethality[22]. Now, S1R antagonism is recognized as a well-grounded opioid adjuvant strategy based on numerous studies reporting antinociceptive enhancement when combining multiple MOR and selective S1R ligands[25,49], and when using opioids in S1R knockout mice[50,51]. Clinical data also

support S1R-mediated modulation of opioid analgesia. Postoperative pain intensity was reported to be reduced when combining a selective S1R antagonist with morphine respect to morphine alone[52]. Patients receiving add-on administration of haloperidol (a potent, albeit non-selective S1R antagonist) also required less opioid administration and rescue therapy to treat abdominal pain than patients treated only with opioids[53]. Supraspinal and peripheral, but not spinal S1R blockade enhanced opioid antinociception[25,51,54]. At the molecular level, S1R physically associates with MOR and this interaction allows S1R ligands to modulate opioid transduction without influencing MOR binding[55,56]. Indeed, S1R is an integral membrane chaperone protein that normally reside at the mitochondrion-associated endoplasmic reticulum membrane, but when cells are stimulated or undergo stress it translocates to the endoplasmic reticulum reticular network and plasma membrane to regulate a variety of receptors and ion channels[57,58]. S1R activation increased the interaction of S1R with GPCRs at the cell surface and inhibit GPCR signalling[59]. Accordingly, S1R ligands work as allosteric modulators of MOR function, S1R antagonists blocking tonic inhibition exerted by S1R in the heteromeric complex[56].

The antinociceptive activity of WLB-73502 in comparison with morphine and oxycodone was explored in several rat pain models. The increase of mechanical (paw pressure) and thermal (tail-flick) nociceptive thresholds is characteristic of opioids. Dose−response curves demonstrated that WLB-73502 had similar potency to oxycodone and near 4-fold more potency than morphine in reducing both thermal and mechanical nociception. This is not surprising, despite its partial MOR agonist activity, taking into consideration its bivalent nature. S1R antagonists lack activity in acute nociception when administered alone but enhanced opioid-induced thermal[23] and mechanical[50] antinociception. The antinociceptive effect of WLB-73502 in the paw pressure test in mice was partially reverted by the co-administration of the S1R agonist PRE-084, and blocked when co-administered with the MOR antagonist naloxone[28], thus supporting the S1R-mediated enhancement of MOR analgesia.

Maximal efficacy after single administration was also achieved by WLB-73502 in reducing mechanical hypersensitivity in carrageenan-induced inflammatory, MIA-induced OA and SNI-induced neuropathic pain models. Potency was similar to oxycodone and 2-fold superior to morphine in inflammatory and OA pain, but superior to both oxycodone (3-fold) and morphine (8-fold) in the neuropathic pain model. Here, besides potentiation of its opioid activity, the contribution *per se* of the non-opioid S1R component of WLB-73502 needs to be considered. Unlike opioids, S1R antagonists do not modify the normal sensory mechanical and thermal perception thresholds but they exert antiallodynic and antihyperalgesic effects in sensitizing conditions (*i.e.*, nerve injury), enabling the reversal of diminished nociceptive thresholds back to normal values[25,60]. Studies in S1R knockout mice[61,62] and using S1R antagonists[62−66] have consistently demonstrated antiallodynic and antihyperalgesic effects. Not only behavioural but also electrophysiological (inhibition of spinal wind-up and nerve injury-induced enhanced axonal activity in peripheral recordings)[66,67], neurochemical (increased noradrenaline but reduced glutamate release in the spinal dorsal horn)[68] and molecular (downregulation of spinal NMDAR function)[69] studies support a role for S1R antagonists in inhibiting augmented excitability secondary to sustained afferent nociceptive input. Thus, especially in partially opioid-refractory pain such as neuropathic pain[70], where stand-alone opioids including morphine and oxycodone required higher doses to exert antinociception, the activity of WLB-73502 likely benefits more from its bivalent inhibitory activity on S1R.

Repeated administration of opioid analgesics results in pharmacodynamic tolerance. Tolerance to the antiallodynic effect of WLB-73502 did not develop in the OA pain model following repeated b.i.d. administration for 28 days at active doses (0.5−3 mg/kg). Time-dependent accumulation of WLB-73502 during repeated administration was discarded as plasma concentration−response curves revealed no differences in $EC_{50}$ values between Day 1 and Day 28. In contrast to WLB-73502, tolerance developed with opioid comparators (morphine and oxycodone), their antiallodynic effect almost disappearing after dosing for 21 days. Tolerance has been reported both for full and partial (and biased) agonists such as buprenorphine[71]; and it was described to develop, or not, or depending on MOR numbers in the case of partial, biased MOR agonist such as SR-17018, PZM21 or TRV-130[72−75]. Knockout mice lacking $\beta$-arrestin-2 failed to develop antinociceptive tolerance after chronic morphine treatment in one first study[76], but morphine tolerance was reported to develop, with a delayed onset and to a lesser degree than in wild-type mice in a second study[77]. The low intrinsic activity at MOR including undetected $\beta$-arrestin recruitment by WLB-73502 could thus explain why tolerance did not develop. However, its antagonistic activity at S1R probably offers a more plausible explanation. Repeated administration of S1R antagonists in combination with opioids disrupt or delay opioid tolerance in numerous pain models, including neuropathic[78], inflammatory[27] and OA[79] pain. Moreover, when administered to morphine-tolerant mice, S1R antagonists rescued opioid analgesia[23,27,80]. Among mechanisms underlying opioid tolerance, the involvement of *N*-methyl-D-aspartate receptors (NMDAR) and modulation of the crosstalk between MOR and NMDAR (*i.e.*, anti-opioid glutamate/NMDAR system) seem the most plausible mechanisms for a S1R antagonist to inhibit opioid tolerance[81−83]. Repeated opioid treatment activates pain facilitatory pathways through specific phosphorylation of NMDAR that limit opioid analgesia[83−85]. In turn, activated NMDAR stimulates kinase cascades that phosphorylate MOR and disrupt its coupling to G-proteins, which also limits opioid analgesia during tolerance development[83,85]. Indeed, tolerance to opioid-analgesia is prevented by inhibiting NMDAR[82,86], and that is what S1R antagonists indirectly do. S1R binds to the C-terminal part of NR1 subunit of NMDAR at a site precluding the binding of calcium−calmodulin, the negative regulator of NMDAR function. When a S1R antagonist binds to S1R, the affinity of S1R for the NR1 subunit of NMDAR diminishes, S1R detaches and allows the entrance of calcium−calmodulin, that inhibit NMDAR, this reducing excitatory nociceptive transmission and the detrimental signalling from NMDAR to MOR[80].

Opioid-induced side effects may be dose-limiting, thus affecting pain control, and reduce patients' quality of life. Constipation is one of the most common (approximately 40% of opioid users) debilitating side effects of opioids[87,88]. Nausea and vomiting are also common opioid-induced gastrointestinal adverse effects (40% of patients may experience nausea and 15%−25% vomiting), highly distressing and often leading to poor adherence to opioid therapy[89]. Respiratory depression is also common but often under-diagnosed in patients receiving opioid analgesia and it is regarded as the main hazard of opioid use by clinicians[90]. It results in excessive sedation and respiratory impairment only in 0.5% or less of the cases, but fatalities are regularly reported[91].

WLB-73502 did not induce gastrointestinal transit inhibition or respiratory depression at doses exerting full antinociceptive effect in rats (5 mg/kg). At higher doses it induced partial intestinal transit inhibition and its effect on respiratory depression reached a plateau of ~30% reduction, with no differences between the 10 and 20 mg/kg doses. In contrast, oxycodone induced remarkable/maximal inhibitory effects on intestinal transit and lung ventilation at doses overlapping those required for analgesia. Similarly, and contrary to morphine, WLB-73502 did not induce emetic response (retching or vomiting) in ferrets at doses that largely exceed the exposure needed to achieve analgesia in rats (*i.e.*, AUC was 18-fold higher in ferrets dosed at 1 mg/kg for the emesis study than in rats receiving 3 mg/kg, a dose active in antinociceptive studies), suggesting that analgesia by WLB-73502 would be achievable also in ferrets without accompanying emesis. In the case of morphine, plasma exposure known to be associated with antinociception in rats[92] exceeds the exposure attained in ferrets[93] dosed similarly to this study, supporting overlapping of the proemetic and analgesic effects of morphine. Reduced respiratory depression, constipation, vomiting and need for rescue antiemetics, and reinforcing activity were reported for biased MOR agonists[44,94,95]. Favourable oliceridine safety profile over morphine when considering emesis[96] and respiratory depression[97] was also reported in human. But other studies applying genetic[98,99], pharmacological[72] or mixed[100,101] approaches reported severe adverse effects associated with G-protein biased MOR agonists. Thus, it is unclear if no/reduced efficacy for $\beta$-arrestin-2 recruitment by WLB-73502 accounts for its improved side effect profile. Its low intrinsic activity at MOR together with its antagonistic activity at S1R may also explain its improved safety. S1R blocking is known to inhibit opioid-induced intestinal transit inhibition, sedation, mydriasis (mice) or lethality[22,23,51,78], and reduced respiratory depression compared to fentanyl at equianalgesic dose was reported with a bifunctional S1R/MOR piperidinamide derivative[102]. S1R has also been involved in the control of emesis: agonists enhance whereas S1R antagonists inhibit emetic response[103]. Interestingly, a reduction of pain and opioid-related side effects, including nausea, vomiting and need for concomitant antiemetic medication was found in the clinic, when comparing the combination of a selective S1R antagonist S1RA (E-52862; MR309) plus morphine with morphine alone in the acute postoperative setting[52].

Addiction is a major drawback of opioids. Apparently, analgesia, rewarding and dependence come together as they all depend upon actions at MOR mainly through the G-protein/cAMP second messenger pathway[104]. The role played by the $\beta$-arrestin pathway here, if any, is unclear[13,72,73,105,106]. We did not evaluate rewarding, tolerance to reward or dependence in this study. WLB-73502 has low intrinsic efficacy at MOR, which would be potentially associated with reduced abuse potential respect to full MOR agonists. Its bivalent S1R antagonism could also potentially contribute due to the opioid-sparing effect (*i.e.*, reduction of opioid load while maintaining efficacy). The reduced effect on respiratory depression would potentially reduce the risk for overdose. As it regards to dependence, we previously published that, contrary to oxycodone, naloxone-precipitated withdrawal signs were not detected following repeated b.i.d. administration of WLB-73502 for 10 days in mice[28]. Finally, S1R antagonists have been proposed as medications for drug abuse as they inhibit rewarding by opioids[23] and other abused substances including cocaine, methamphetamine, ethanol, and nicotine[107–109]. Opioid addiction is a truly sensitive and delicate matter. Further studies are warranted.

Target engagement supports activity findings. When administered systemically (i.p.), WLB-73502 crossed the BBB (higher exposure in brain than in plasma) and, according to its bivalent nature, bound to both brain MOR and S1R. Preliminary PK/PD analysis revealed a consistency between brain exposure, MOR and S1R affinities, brain MOR and S1R occupancy, and antinociceptive efficacy. Efficacy *in vivo* at 3 mg/kg (average 75%) was a bit higher than expected based on a direct translation of receptor occupancies obtained by *ex vivo* autoradiography (average 50 and 60% for MOR and S1R, respectively). Non-exact linear correspondence (*i.e.*, slope $\neq$ 1) between the cause (binding to receptors) and the effect (antinociceptive response) is not surprising, particularly if a superior effect is expected when both S1R and MOR are recruited.

## 5. Conclusions

WLB-73502 is a bispecific S1R antagonist and MOR partial agonist with analgesia comparable (nociceptive and mixed inflammatory and OA pain) or superior (neuropathic pain) to full MOR agonists, but it does not induce tolerance and causes no/less constipation, respiratory depression, and nausea/vomiting than strong opioids. WLB-73502 benefits from its partial MOR agonist nature (low intrinsic efficacy at $G_{i/o}$-protein activation and undetectable $\beta$-arrestin-2 recruitment) and its bivalent S1R antagonist activity, responsible for opioid-dependent and -independent effects, to increase its therapeutic index. This makes WLB-73502 a promising alternative for treating chronic refractory pain, potentially neuropathic cancer pain, where regular stand-alone opioids do not achieve satisfactory outcomes and are limited by drug tolerance and adverse effects[110]. In agreement with findings with WLB-73502, other bifunctional S1R antagonist/MOR agonist derivatives including piperidinamides[102], benzylpiperazines[111] and 4-aryl-1-oxa-4,9-diazaspiro[5.5]undecanes[112] also produced fewer opioid-like side effects, thus highlighting dual S1R antagonism/MOR agonism as a hopeful avenue for the development of potent and safer analgesics[113].

## Acknowledgments

The present study was partially supported by the Centre for the Development of Industrial Technology (Centro para el Desarrollo Tecnológico Industrial; CDTI), references IDI-20130943 and IDI-20150915 (Spain).

## Author contributions

Begoña Fernández-Pastor, Manuel Merlos and José Miguel Vela conceived the study; Javier Burgueño, Xavier Codony, Maria Teresa Serafini, Gregorio Encina and Daniel Zamanillo proposed the methods and directed the studies; Alba Vidal-Torres, Eva Ayet, Anna Cabot, Xavier Monroy and Bertrand Aubel conducted the experiments, analysed the data and wrote parts of the initial draft; Luz Romero analysed the data; Alba Vidal-Torres and Luz Romero did the charts and focused on data presentation; Alba Vidal-Torres, Begoña Fernández-Pastor and José Miguel Vela

wrote the manuscript; Rosalía Pascual generated 3D-models of MOR and S1R with the docked WLB-73502, displayed in the graphical abstract; and Mónica García, Luz Romero, Carmen Almansa and Manuel Merlos revised the manuscript. José Miguel Vela was responsible for ensuring that the descriptions are accurate and agreed by all authors. All authors reviewed the manuscript and approved the final version.

## Conflicts of interest

The authors are full-time employees in Welab Barcelona.

## Appendix A. Supporting information

Supporting data to this article can be found online at https://doi.org/10.1016/j.apsb.2022.09.018.

## References


1. Cohen SP, Vase L, Hooten WM. Chronic pain: an update on burden, best practices, and new advances. *Lancet* 2021;**397**:2082–97.
2. Mercadante S. Opioid analgesics adverse effects: the other side of the coin. *Curr Pharmaceut Des* 2019;**25**:3197–202.
3. Zhou J, Ma R, Jin Y, Fang J, Du J, Shao X, et al. Molecular mechanisms of opioid tolerance: from opioid receptors to inflammatory mediators (Review). *Exp Ther Med* 2021;**22**:1004.
4. Gardner EA, McGrath SA, Dowling D, Bai D. The opioid crisis: prevalence and markets of opioids. *Forensic Sci Rev* 2022;**34**:43–70.
5. Busserolles J, Lolignier S, Kerckhove N, Bertin C, Authier N, Eschalier A. Replacement of current opioid drugs focusing on MOR-related strategies. *Pharmacol Ther* 2020;**210**:107519.
6. Gillis A, Gondin AB, Kliewer A, Sanchez J, Lim HD, Alamein C, et al. Low intrinsic efficacy for G protein activation can explain the improved side effect profiles of new opioid agonists. *Sci Signal* 2020;**13**:eaaz3140.
7. Zuurmond WW, Meert TF, Noorduin H. Partial versus full agonists for opioid-mediated analgesia—focus on fentanyl and buprenorphine. *Acta Anaesthesiol Belg* 2002;**53**:193–201.
8. Pergolizzi JV, Raffa RB. Safety and efficacy of the unique opioid buprenorphine for the treatment of chronic pain. *J Pain Res* 2019;**12**:3299–317.
9. Hale M, Garofoli M, Raffa RB. Benefit-risk analysis of buprenorphine for pain management. *J Pain Res* 2021;**14**:1359–69.
10. Smith JS, Lefkowitz RJ, Rajagopal S. Biased signalling: from simple switches to allosteric microprocessors. *Nat Rev Drug Discovery* 2018;**17**:243–60.
11. De Neve J, Barlow TMA, Tourwé D, Bihel F, Simonin F, Ballet S. Comprehensive overview of biased pharmacology at the opioid receptors: biased ligands and bias factors. *RSC Med Chem* 2021;**12**:828–70.
12. Hammer GB, Khanna AK, Michalsky C, Wase L, Demitrack MA, Little R, et al. Oliceridine exhibits improved tolerability compared to morphine at equianalgesic conditions: exploratory analysis from two phase 3 randomized placebo and active controlled trials. *Pain Ther* 2021;**10**:1343–53.
13. Negus SS, Freeman KB. Abuse potential of biased mu opioid receptor agonists. *Trends Pharmacol Sci* 2018;**39**:916–9.
14. Tan HS, Habib AS. Safety evaluation of oliceridine for the management of postoperative moderate-to-severe acute pain. *Expet Opin Drug Saf* 2021;**20**:1291–8.
15. Smith HS. Combination opioid analgesics. *Pain Physician* 2008;**11**:201–14.
16. Bihel F. Opioid adjuvant strategy: improving opioid effectiveness. *Future Med Chem* 2016;**8**:339–54.
17. Sawaddiruk P. Tramadol hydrochloride/acetaminophen combination for the relief of acute pain. *Drugs Today* 2011;**47**:763–72.
18. Merlos M, Portillo-Salido E, Brenchat A, Aubel B, Buxens J, Fisas A, et al. Administration of a co-crystal of tramadol and celecoxib in a 1:1 molecular ratio produces synergistic antinociceptive effects in a postoperative pain model in rats. *Eur J Pharmacol* 2018;**833**:370–8.
19. Almansa C, Frampton CS, Vela JM, Whitelock S, Plata-Salamán CR. Co-crystals as a new approach to multimodal analgesia and the treatment of pain. *J Pain Res* 2019;**12**:2679–89.
20. Raffa RB, Elling C, Tzschentke TM. Does 'strong analgesic' equal 'strong opioid'? Tapentadol and the concept of '$\mu$-Load'. *Adv Ther* 2018;**35**:1471–84.
21. Morphy R, Rankovic Z. Designed multiple ligands. An emerging drug discovery paradigm. *J Med Chem* 2005;**48**:6523–43.
22. Chien CC, Pasternak GW. Selective antagonism of opioid analgesia by a sigma system. *J Pharmacol Exp Therapeut* 1994;**271**:1583–90.
23. Vidal-Torres A, de la Puente B, Rocasalbas M, Touriño C, Bura SA, Fernández-Pastor B, et al. Sigma-1 receptor antagonism as opioid adjuvant strategy: enhancement of opioid antinociception without increasing adverse effects. *Eur J Pharmacol* 2013;**711**:63–72.
24. Zamanillo D, Romero L, Merlos M, Vela JM. Sigma 1 receptor: a new therapeutic target for pain. *Eur J Pharmacol* 2013;**716**:78–93.
25. Romero L, Merlos M, Vela JM. Antinociception by sigma-1 receptor antagonists: central and peripheral effects. *Adv Pharmacol* 2016;**75**:179–215.
26. Sánchez-Fernández C, Entrena JM, Baeyens JM, Cobos EJ. Sigma-1 receptor antagonists: a new class of neuromodulatory analgesics. *Adv Exp Med Biol* 2017;**964**:109–32.
27. Montilla-García Á, Tejada MÁ, Ruiz-Cantero MC, Bravo-Caparrós I, Yeste S, Zamanillo D, et al. Modulation by sigma-1 receptor of morphine analgesia and tolerance: nociceptive pain, tactile allodynia and grip strength deficits during joint inflammation. *Front Pharmacol* 2019;**10**:136.
28. García M, Virgili M, Alonso M, Alegret C, Farran J, Fernández B, et al. Discovery of EST73502, a dual $\mu$-opioid receptor agonist and $\sigma$1 receptor antagonist clinical candidate for the treatment of pain. *J Med Chem* 2020;**63**:15508–26.
29. Cobos EJ, Baeyens JM, Del Pozo E. Phenytoin differentially modulates the affinity of agonist and antagonist ligands for sigma 1 receptors of Guinea pig brain. *Synapse* 2005;**55**:192–5.
30. Zimmermann M. Ethical guidelines for investigations of experimental pain in conscious animals. *Pain* 1983;**16**:109–10.
31. Percie du Sert N, Hurst V, Ahluwalia A, Alam S, Avey MT, Baker M, et al. The ARRIVE guidelines 2.0: updated guidelines for reporting animal research. *Br J Pharmacol* 2020;**177**:3617–24.
32. Randall LO, Selitto JJ. A method for measurement of analgesic activity on inflamed tissue. *Arch Int Pharmacodyn Ther* 1957;**111**:409–19.
33. D'amour FE, Smith DL. A method for determining loss of pain sensation. *J Pharmacol Exp Therapeut* 1941;**72**:74–9.
34. Winter CA, Risley EA, Nuss GW. Carrageenin-induced edema in hind paw of the rat as an assay for antiiflammatory drugs. *Proc Soc Exp Biol Med* 1962;**111**:544–7.
35. Dunham J, Hoedt-Schmidt S, Kalbhen DA. Prolonged effect of iodoacetate on articular cartilage and its modification by an antirheumatic drug. *Int J Exp Pathol* 1993;**74**:283–9.
36. Decosterd I, Woolf CJ. Spared nerve injury: an animal model of persistent peripheral neuropathic pain. *Pain* 2000;**87**:149–58.
37. Burgueño J, Pujol M, Monroy X, Roche D, Varela MJ, Merlos M, et al. A complementary scale of biased agonism for agonists with differing maximal responses. *Sci Rep* 2017;**7**:15389.

38. Nickolls SA, Waterfield A, Williams RE, Kinloch RA. Understanding the effect of different assay formats on agonist parameters: a study using the μ-opioid receptor. *J Biomol Screen* 2011;**16**:706−16.
39. Arvidsson U, Riedl M, Chakrabarti S, Lee JH, Nakano AH, Dado RJ, et al. Distribution and targeting of a mu-opioid receptor (MOR1) in brain and spinal cord. *J Neurosci* 1995;**15**:3328−41.
40. Alonso G, Phan V, Guillemain I, Saunier M, Legrand A, Anoal M, et al. Immunocytochemical localization of the sigma$_1$ receptor in the adult rat central nervous system. *Neuroscience* 2000;**97**:155−70.
41. Ayet E, Yeste S, Reinoso RF, Pretel MJ, Balada A, Serafini MT. Preliminary *in vitro* approach to evaluate the drug−drug interaction potential of EST73502, a dual μ-opioid receptor partial agonist and σ1 receptor antagonist. *Xenobiotica* 2021;**51**:501−12.
42. Goineau S, Castagné V. Comparison of three preclinical models for nausea and vomiting assessment. *J Pharmacol Toxicol Methods* 2016;**82**:45−53.
43. DeWire SM, Ahn S, Lefkowitz RJ, Shenoy SK. Beta-arrestins and cell signaling. *Annu Rev Physiol* 2007;**69**:483−510.
44. DeWire SM, Yamashita DS, Rominger DH, Liu G, Cowan CL, Graczyk TM, et al. A G protein-biased ligand at the μ-opioid receptor is potently analgesic with reduced gastrointestinal and respiratory dysfunction compared with morphine. *J Pharmacol Exp Therapeut* 2013;**344**:708−17.
45. Azevedo Neto J, Costanzini A, De Giorgio R, Lambert DG, Ruzza C, Calò G. Biased *versus* partial agonism in the search for safer opioid analgesics. *Molecules* 2020;**25**:E3870.
46. Gillis A, Sreenivasan V, Christie MJ. Intrinsic efficacy of opioid ligands and its importance for apparent bias, operational analysis, and therapeutic window. *Mol Pharmacol* 2020;**98**:410−24.
47. Stahl EL, Bohn LM. Low intrinsic efficacy alone cannot explain the improved side effect profiles of new opioid agonists. *Biochemistry* 2022;**61**:1923−35.
48. Chien CC, Pasternak GW. Functional antagonism of morphine analgesia by (+)-pentazocine: evidence for an anti-opioid sigma 1 system. *Eur J Pharmacol* 1993;**250**:R7−8.
49. Vela JM, Merlos M, Almansa C. Investigational sigma-1 receptor antagonists for the treatment of pain. *Expet Opin Invest Drugs* 2015;**24**:883−96.
50. Sánchez-Fernández C, Nieto FR, González-Cano R, Artacho-Cordón A, Romero L, Montilla-García Á, et al. Potentiation of morphine-induced mechanical antinociception by $\sigma_1$ receptor inhibition: role of peripheral $\sigma_1$ receptors. *Neuropharmacology* 2013;**70**:348−58.
51. Sánchez-Fernández C, Montilla-García Á, González-Cano R, Nieto FR, Romero L, Artacho-Cordón A, et al. Modulation of peripheral μ-opioid analgesia by σ1 receptors. *J Pharmacol Exp Therapeut* 2014;**348**:32−45.
52. Sust M, Montes A, Morte A, Domingo-Triado V, Manrique S, Martínez A, et al. E-52862, a first-in-class sigma-1 receptor antagonist, in acute post-operative pain following open abdominal hysterectomy. An exploratory phase II clinical trial. In: Abstract 2738, Yokohama, Japan: IASP 2016; 2016, p. Poster ID PTH 283. 16 th World Congress of pain. IASP Sept 26-30; 2016. Last accessed June 15, 2022. Available from: https://event.crowdcompass.com/wcp2016/activity/twXasfd7DT.
53. Knudsen-Lachendro K, Stith K, Vicarel LA, Harbert B, Fertel BS. Study of haloperidol for abdominal pain in the emergency department (SHAPE). *West J Emerg Med* 2021;**22**:623−7.
54. Vidal-Torres A, Fernández-Pastor B, Carceller A, Vela JM, Merlos M, Zamanillo D. Supraspinal and peripheral, but not intrathecal, σ1R blockade by S1RA enhances morphine antinociception. *Front Pharmacol* 2019;**10**:422.
55. Kim FJ, Kovalyshyn I, Burgman M, Neilan C, Chien CC, Pasternak GW. Sigma 1 receptor modulation of G-protein-coupled receptor signaling: potentiation of opioid transduction independent from receptor binding. *Mol Pharmacol* 2010;**77**:695−703.
56. Pasternak GW. Allosteric modulation of opioid G-protein coupled receptors by sigma1 receptors. *Handb Exp Pharmacol* 2017;**244**:163−75.
57. Su T-P, Hayashi T, Maurice T, Buch S, Ruoho AE. The sigma-1 receptor chaperone as an inter-organelle signaling modulator. *Trends Pharmacol Sci* 2010;**31**:557−66.
58. Kim FJ. Introduction to sigma proteins: evolution of the concept of sigma receptors. *Handb Exp Pharmacol* 2017;**244**:1−11.
59. Aguinaga D, Medrano M, Cordomí A, Jiménez-Rosés M, Angelats E, Casanovas M, et al. Cocaine blocks effects of hunger hormone, ghrelin, *via* interaction with neuronal sigma-1 receptors. *Mol Neurobiol* 2019;**56**:1196−210.
60. Merlos M, Burgueño J, Portillo-Salido E, Plata-Salamán CR, Vela JM. Pharmacological modulation of the sigma 1 receptor and the treatment of pain. *Adv Exp Med Biol* 2017;**964**:85−107.
61. De la Puente B, Nadal X, Portillo-Salido E, Sánchez-Arroyos R, Ovalle S, Palacios G, et al. Sigma-1 receptors regulate activity-induced spinal sensitization and neuropathic pain after peripheral nerve injury. *Pain* 2009;**145**:294−303.
62. Nieto FR, Cendán CM, Cañizares FJ, Cubero MA, Vela JM, Fernández-Segura E, et al. Genetic inactivation and pharmacological blockade of sigma-1 receptors prevent paclitaxel-induced sensory-nerve mitochondrial abnormalities and neuropathic pain in mice. *Mol Pain* 2014;**10**:11.
63. Romero L, Zamanillo D, Nadal X, Sánchez-Arroyos R, Rivera-Arconada I, Dordal A, et al. Pharmacological properties of S1RA, a new sigma-1 receptor antagonist that inhibits neuropathic pain and activity-induced spinal sensitization. *Br J Pharmacol* 2012;**166**:2289−306.
64. Gris G, Merlos M, Vela JM, Zamanillo D, Portillo-Salido E. S1RA, a selective sigma-1 receptor antagonist, inhibits inflammatory pain in the carrageenan and complete Freund's adjuvant models in mice. *Behav Pharmacol* 2014;**25**:226−35.
65. Gris G, Portillo-Salido E, Aubel B, Darbaky Y, Deseure K, Vela JM, et al. The selective sigma-1 receptor antagonist E-52862 attenuates neuropathic pain of different aetiology in rats. *Sci Rep* 2016;**6**:24591.
66. Paniagua N, Girón R, Goicoechea C, López-Miranda V, Vela JM, Merlos M, et al. Blockade of sigma 1 receptors alleviates sensory signs of diabetic neuropathy in rats. *Eur J Pain* 2017;**21**:61−72.
67. Mazo I, Roza C, Zamanillo D, Merlos M, Vela JM, Lopez-Garcia JA. Effects of centrally acting analgesics on spinal segmental reflexes and wind-up. *Eur J Pain* 2015;**19**:1012−20.
68. Vidal-Torres A, Fernández-Pastor B, Carceller A, Vela JM, Merlos M, Zamanillo D. Effects of the selective sigma-1 receptor antagonist S1RA on formalin-induced pain behavior and neurotransmitter release in the spinal cord in rats. *J Neurochem* 2014;**129**:484−94.
69. Kim HW, Roh DH, Yoon SY, Seo HS, Kwon YB, Han HJ, et al. Activation of the spinal sigma-1 receptor enhances NMDA-induced pain *via* PKC- and PKA-dependent phosphorylation of the NR1 subunit in mice. *Br J Pharmacol* 2008;**154**:1125−34.
70. Martínez-Navarro M, Maldonado R, Baños JE. Why mu-opioid agonists have less analgesic efficacy in neuropathic pain?. *Eur J Pain* 2019;**23**:435−54.
71. Larson CM, Peterson CD, Kitto KF, Wilcox GL, Fairbanks CA. Sustained-release buprenorphine induces acute opioid tolerance in the mouse. *Eur J Pharmacol* 2020;**885**:173330.
72. Altarifi AA, David B, Muchhala KH, Blough BE, Akbarali H, Negus SS. Effects of acute and repeated treatment with the biased mu opioid receptor agonist TRV130 (oliceridine) on measures of antinociception, gastrointestinal function, and abuse liability in rodents. *J Psychopharmacol* 2017;**31**:730−9.
73. Kudla L, Bugno R, Skupio U, Wiktorowska L, Solecki W, Wojtas A, et al. Functional characterization of a novel opioid, PZM21, and its effects on the behavioural responses to morphine. *Br J Pharmacol* 2019;**176**:4434−45.
74. Grim TW, Schmid CL, Stahl EL, Pantouli F, Ho JH, Acevedo-Canabal A, et al. A G protein signaling-biased agonist at the μ-opioid receptor reverses morphine tolerance while preventing morphine withdrawal. *Neuropsychopharmacology* 2020;**45**:416−25.
75. Singleton S, Baptista-Hon DT, Edelsten E, McCaughey KS, Camplisson E, Hales TG. TRV130 partial agonism and capacity to

induce anti-nociceptive tolerance revealed through reducing available $\mu$-opioid receptor number. *Br J Pharmacol* 2021;**178**:1855−68.
76. Bohn LM, Gainetdinov RR, Lin FT, Lefkowitz RJ, Caron MG. $\mu$-Opioid receptor desensitization by beta-arrestin-2 determines morphine tolerance but not dependence. *Nature* 2000;**408**:720−3.
77. Bohn LM, Lefkowitz RJ, Caron MG. Differential mechanisms of morphine antinociceptive tolerance revealed in $\beta$arrestin-2 knock-out mice. *J Neurosci* 2002;**22**:10494−500.
78. Mena-Valdés LC, Blanco-Hernández Y, Espinosa-Juárez JV, López-Muñoz FJ. Haloperidol potentiates antinociceptive effects of morphine and disrupt opioid tolerance. *Eur J Pharmacol* 2021;**893**:173825.
79. Carcolé M, Kummer S, Gonçalves L, Zamanillo D, Merlos M, Dickenson AH, et al. Sigma-1 receptor modulates neuroinflammation associated with mechanical hypersensitivity and opioid tolerance in a mouse model of osteoarthritis pain. *Br J Pharmacol* 2019;**176**:3939−55.
80. Rodríguez-Muñoz M, Sánchez-Blázquez P, Herrero-Labrador R, Martínez-Murillo R, Merlos M, Vela JM, et al. The $\sigma$1 receptor engages the redox-regulated HINT1 protein to bring opioid analgesia under NMDA receptor negative control. *Antioxidants Redox Signal* 2015;**22**:799−818.
81. Mao J. NMDA and opioid receptors: their interactions in antinociception, tolerance and neuroplasticity. *Brain Res Brain Res Rev* 1999;**30**:289−304.
82. Price DD, Mayer DJ, Mao J, Caruso FS. NMDA-receptor antagonists and opioid receptor interactions as related to analgesia and tolerance. *J Pain Symptom Manag* 2000;**19**:S7−11.
83. Garzón J, Rodríguez-Muñoz M, Sánchez-Blázquez P. Direct association of mu-opioid and NMDA glutamate receptors supports their cross-regulation: molecular implications for opioid tolerance. *Curr Drug Abuse Rev* 2012;**5**:199−226.
84. Hsu MM, Wong CS. The roles of pain facilitatory systems in opioid tolerance. *Acta Anaesthesiol Sin* 2000;**38**:155−66.
85. Sánchez-Blázquez P, Rodríguez-Muñoz M, Berrocoso E, Garzón J. The plasticity of the association between mu-opioid receptor and glutamate ionotropic receptor N in opioid analgesic tolerance and neuropathic pain. *Eur J Pharmacol* 2013;**716**:94−105.
86. Bespalov AY, Zvartau EE, Beardsley PM. Opioid-NMDA receptor interactions may clarify conditioned (associative) components of opioid analgesic tolerance. *Neurosci Biobehav Rev* 2001;**25**:343−53.
87. Bell T, Annunziata K, Leslie JB. Opioid-induced constipation negatively impacts pain management, productivity, and health-related quality of life: findings from the National Health and Wellness Survey. *J Opioid Manage* 2009;**5**:137−44.
88. Andresen V, Banerji V, Hall G, Lass A, Emmanuel AV. The patient burden of opioid-induced constipation: new insights from a large, multinational survey in five European countries. *United European Gastroenterol J* 2018;**6**:1254−66.
89. Mallick-Searle T, Fillman M. The pathophysiology, incidence, impact, and treatment of opioid-induced nausea and vomiting. *J Am Assoc Nurse Pract* 2017;**29**:704−10.
90. Ayad S, Khanna AK, Iqbal SU, Singla N. Characterisation and monitoring of postoperative respiratory depression: current approaches and future considerations. *Br J Anaesth* 2019;**123**:378−91.
91. Dahan A, Aarts L, Smith TW. Incidence, reversal, and prevention of opioid-induced respiratory depression. *Anesthesiology* 2010;**112**:226−38.
92. Shang G, Liu D, Yan L, Cui X, Zhang K, Qi C, et al. Nociceptive stimulus modality-related difference in pharmacokinetic−pharmacodynamic modeling of morphine in the rat. *Pharmacol Biochem Behav* 2006;**85**:464−73.
93. Kanemasa T, Matsuzaki T, Koike K, Hasegawa M, Suzuki T. Preventive effects of naldemedine, peripherally acting $\mu$-opioid receptor antagonist, on morphine-induced nausea and vomiting in ferrets. *Life Sci* 2020;**257**:118048.
94. Manglik A, Lin H, Aryal DK, McCorvy JD, Dengler D, Corder G, et al. Structure-based discovery of opioid analgesics with reduced side effects. *Nature* 2016;**537**:185−90.
95. Schmid CL, Kennedy NM, Ross NC, Lovell KM, Yue Z, Morgenweck J, et al. Bias factor and therapeutic window correlate to predict safer opioid analgesics. *Cell* 2017;**171**:1165−1175.e13.
96. Beard TL, Michalsky C, Candiotti KA, Rider P, Wase L, Habib AS, et al. Oliceridine is associated with reduced risk of vomiting and need for rescue antiemetics compared to morphine: exploratory analysis from two phase 3 randomized placebo and active controlled trials. *Pain Ther* 2021;**10**:401−13.
97. Dahan A, van Dam CJ, Niesters M, van Velzen M, Fossler MJ, Demitrack MA, et al. Benefit and risk evaluation of biased $\mu$-receptor agonist oliceridine versus morphine. *Anesthesiology* 2020;**133**:559−68.
98. Kliewer A, Schmiedel F, Sianati S, Bailey A, Bateman JT, Levitt ES, et al. Phosphorylation-deficient G-protein-biased $\mu$-opioid receptors improve analgesia and diminish tolerance but worsen opioid side effects. *Nat Commun* 2019;**10**:367.
99. Bachmutsky I, Wei XP, Durand A, Yackle K. $\beta$-Arrestin 2 germline knockout does not attenuate opioid respiratory depression. *Elife* 2021;**10**:e62552.
100. Kliewer A, Gillis A, Hill R, Schmiedel F, Bailey C, Kelly E, et al. Morphine-induced respiratory depression is independent of $\beta$-arrestin2 signalling. *Br J Pharmacol* 2020;**177**:2923−31.
101. Haouzi P, McCann M, Tubbs N. Respiratory effects of low and high doses of fentanyl in control and $\beta$-arrestin 2-deficient mice. *J Neurophysiol* 2021;**125**:1396−407.
102. Xiong J, Zhuang T, Ma Y, Xu J, Ye J, Ma R, et al. Optimization of bifunctional piperidinamide derivatives as $\sigma$1R Antagonists/MOR agonists for treating neuropathic pain. *Eur J Med Chem* 2021;**226**:113879.
103. Hudzik TJ. Sigma ligand-induced emesis in the pigeon. *Pharmacol Biochem Behav* 1992;**41**:215−7.
104. Chao J, Nestler EJ. Molecular neurobiology of drug addiction. *Annu Rev Med* 2004;**55**:113−32.
105. Austin Zamarripa C, Edwards SR, Qureshi HN, Yi JN, Blough BE, Freeman KB. The G-protein biased mu-opioid agonist, TRV130, produces reinforcing and antinociceptive effects that are comparable to oxycodone in rats. *Drug Alcohol Depend* 2018;**192**:158−62.
106. Ding H, Kiguchi N, Perrey DA, Nguyen T, Czoty PW, Hsu FC, et al. Antinociceptive, reinforcing, and pruritic effects of the G-protein signalling-biased mu opioid receptor agonist PZM21 in non-human primates. *Br J Anaesth* 2020;**125**:596−604.
107. Maurice T, Martin-Fardon R, Romieu P, Matsumoto RR. Sigma$_1$ ($\sigma_1$) receptor antagonists represent a new strategy against cocaine addiction and toxicity. *Neurosci Biobehav Rev* 2002;**26**:499−527.
108. Matsumoto RR. Targeting sigma receptors: novel medication development for drug abuse and addiction. *Expet Rev Clin Pharmacol* 2009;**2**:351−8.
109. Robson MJ, Noorbakhsh B, Seminerio MJ, Matsumoto RR. Sigma-1 receptors: potential targets for the treatment of substance abuse. *Curr Pharmaceut Des* 2012;**18**:902−19.
110. Jongen JLM, Huijsman ML, Jessurun J, Ogenio K, Schipper D, Verkouteren DRC, et al. The evidence for pharmacologic treatment of neuropathic cancer pain: beneficial and adverse effects. *J Pain Symptom Manage* 2013;**46**:581−590.e1.
111. Wilson LL, Eans SO, Ramadan-Siraj I, Modica MN, Romeo G, Intagliata S, et al. Examination of the novel sigma-1 receptor antagonist, SI 1/28, for antinociceptive and anti-allodynic efficacy against multiple types of nociception with fewer liabilities of use. *Int J Mol Sci* 2022;**23**:615.
112. García M, Virgili M, Alonso M, Alegret C, Fernández B, Port A, et al. 4-Aryl-1-oxa-4,9-diazaspiro[5.5]undecane derivatives as dual $\mu$-opioid receptor agonists and $\sigma$1 receptor antagonists for the treatment of pain. *J Med Chem* 2020;**63**:2434−54.
113. Zhuang T, Xiong J, Hao S, Du W, Liu Z, Liu B, et al. Bifunctional $\mu$ opioid and $\sigma$1 receptor ligands as novel analgesics with reduced side effects. *Eur J Med Chem* 2021;**223**:113658.